Ligand Binding to Heme Proteins: The Effect of Light on Ligand Binding in Myoglobin†

G. Ulrich Nienhaus,* Judith R. Mourant,‡ Kelvin Chu, and Hans Frauenfelder§

Department of Physics, University of Illinois at Urbana−Champaign, 1110 West Green Street, Urbana, Illinois 61801-3080

Received February 8, 1994; Revised Manuscript Received August 23, 1994⊗

ABSTRACT: Extended illumination slows the rebinding of CO to myoglobin after photodissociation at cryogenic temperatures. Two types of models have been put forward to explain the effect: motions of the CO within the heme pocket or conformational transitions of the protein. To resolve this ambiguity, we have studied the effect of extended illumination on ligand binding to horse and sperm whale myoglobin (hMb and swMb) with temperature-derivative spectroscopy, monitoring the reaction in the CO stretch bands in the infrared and the conformation-sensitive band III near 760 nm. The experiments show that the stretch frequency of the photodissociated CO does not change upon illumination, implying that the slowing of the CO rebinding is caused by conformational relaxation of Mb from the bound state toward the deoxy structure. The light-induced relaxation (LIR) depends on the number of photons absorbed but not on the light intensity or duration separately. LIR occurs on photon absorption in either the bound or photodissociated state and depends on the temperature at which the MbCO is illuminated. The LIR proceeds in jumps through a small number of conformational substates. The effective barrier for rebinding increases with each step. The substates populated are similar to those found in the thermally-induced relaxation (TIR) that is observed above 160 K. LIR depends markedly on the structural details; it differs for swMbCO and hMbCO and even for the three A substates of swMbCO. Pronounced differences exist between the effects in MbCO and MbO_2. The similarity of LIR and TIR leads to a revised model for ligand binding to swMbCO and hMbCO, in which the relaxation is crucial for the escape of the ligand from the pocket, as was first suggested by Friedman [Friedman, J. M. (1985) *Science 228,* 1273−1280].

1. LIGHT SLOWS LIGAND BINDING

Light is essential for life. The effects of light on biological processes have been studied widely, but some aspects are still not fully understood. In the present work, we consider the effect of light on the binding of carbon monoxide (CO) and dioxygen (O_2) to sperm whale and horse myoglobin (swMb and hMb). Haldane and Smith (1896) discovered that carbonmonoxy-hemoglobin is photosensitive: HbCO + $h\nu \rightarrow$ Hb + CO. Such photodissociation processes have by now been studied in great detail. Does the inverse process, ligand binding, change under the influence of light? Brunori and collaborators showed in 1972 that the rate coefficient for CO binding is not affected by light at room temperature (Brunori et al., 1972; Bonaventura et al., 1973). This result appears to be reasonable. Photodissociation has a clear physical basis: A photon breaks the bond between the heme iron and the bound CO. No such straightforward mechanism is obvious for an effect of light on ligand association. It came therefore as a surprise when Chance and collaborators found in 1986 that continuous illumination can slow CO rebinding at cryogenic temperatures (Chance et al., 1986; Powers et al., 1987). They coined the term "pumping" for this effect. This result has been verified by various groups (Ansari et al., 1987; Winkler et al., 1990; Šrajer et al., 1991; Ahmed et al., 1991). Similar effects had already been observed in the electron-transfer kinetics in photosynthetic reaction centers (Noks et al., 1977; Kleinfeld et al., 1984).

Various explanations for the slowing have been proposed. Powers and collaborators (1987) suggested that there are discrete way stations or docking sites along the ligand-binding pathway and that light pumps the system from faster to slower binding sites. Ansari et al. (1987) attributed the slowing to rare thermal transitions into longer-lived conformational substates (CS) as the protein−ligand systems are kept photodissociated. Champion and collaborators (Šrajer et al., 1991) introduced a four-state model with two geminate states. Friedman and collaborators (Ahmed et al., 1991) studied the temperature dependence of the resonance Raman spectra of MbCO and noticed changes in the Fe−His stretching mode that depend on light intensity and illumination time. They favored an explanation in terms of conformational changes of the protein molecule, in particular on the proximal side.

The models for the effect of light on the CO binding kinetics fall into two classes, stressing either the CO position (Powers et al., 1987; Šrajer et al., 1991) or the protein conformation (Ansari et al., 1987; Ahmed et al., 1991). In the first class, the protein maintains its structure and light pumps the ligands to alternative sites along the reaction pathway from which they rebind more slowly. In the second class, light modifies the protein structure and the protein relaxes into conformational substates with slower rebinding.

† This is the fourth paper in a series on ligand binding to heme proteins. The work was supported in part by the National Institutes of Health (Grants GM 18051), the Office of Naval Research (Grant N 00014-92-J-1941), and the National Science Foundation (Grant DMB87-16476).

‡ Present address: MS E535, CLS-5, Los Alamos National Laboratory, Los Alamos, NM 87545.

§ Permanent address: MS M715, P-6, Los Alamos National Laboratory, Los Alamos, NM 87545.

⊗ Abstract published in *Advance ACS Abstracts,* October 15, 1994.

0006-2960/94/0433-13413$04.50/0

The division into two classes is, of course, not as sharp as drawn here. A conformational change, induced by light, can affect the structure of the heme pocket and hence change the position of the photodissociated CO. Low-temperature X-ray structure analysis (Schlichting et al., 1994) of the photodissociated state without and with extended illumination will be performed to address this issue.

In the present paper, we study the light effect by using two different structure-sensitive spectroscopic markers. The infrared stretch bands of the bound and photodissociated CO are superb probes for monitoring the kinetics of CO binding to the three A substrates individually (Ansari et al., 1987). Furthermore, the CO stretch bands are sensitive to the environment and can monitor structural changes and CO motions in the heme pocket. The near-IR band III at ~760 nm is a sensitive marker for the protein structure near the heme group (Iizuka et al., 1974; Steinbach et al., 1991; Nienhaus et al., 1992). Combined use of the two markers leads us to conclude that "pumping" is *not* caused by motion of the CO to sites from where it rebinds more slowly but by conformational changes (light-induced relaxation, LIR) that increase the barrier for rebinding to the heme iron.

2. BACKGROUND

The model and approach underlying the present work have been described in detail in earlier papers (Austin et al., 1975; Ansari et al., 1987; Steinbach et al., 1991; Mourant et al., 1993). Five results are important for the following discussions:

(i) Below ~160 K, the photodissociated ligand does not escape from the protein but rebinds from within the heme pocket. The simplest kinetic scheme invokes two states, A and B. In A, the CO is bound to the heme iron (MbCO). In B, the photodissociated CO is in the heme pocket, from where it can rebind by overcoming a barrier between the states B and A.

(ii) Rebinding is nonexponential in time. The time and temperature dependence of the rebinding between about 60 and 160 K can be described with a temperature-independent distribution, $g(H_{BA})$, of activation enthalpies (Austin et al., 1975; Frauenfelder et al., 1988). The survival probability is then given by

$$N(t) = \int g(H_{BA}) e^{-k_{BA}t}\, dH_{BA} \qquad (1)$$

Here $g(H_{BA})\, dH_{BA}$ is the probability of finding a barrier between H_{BA} and $H_{BA} + dH_{BA}$. Neglecting tunneling transitions, the rebinding rate coefficient, k_{BA}, is given by the transition-state expression (Dlott et al., 1983)

$$k_{BA} = A_{BA}(T/T_0) e^{-H_{BA}/RT} \qquad (2)$$

with the reference temperature $T_0 = 100$ K and the pre-exponential $A_{BA} \simeq 10^9\ s^{-1}$ for swMbCO.

(iii) The nonexponential rebinding is caused by conformational substates (CS): A protein with a given primary sequence can assume a very large number of slightly different conformations (Austin et al., 1975; Frauenfelder et al., 1988, 1991). Below about 160 K, thermal transitions between CS do not occur; each molecule is frozen into a particular CS.

(iv) Conformational substates are organized hierarchically (Ansari et al., 1985, 1987; Frauenfelder et al., 1991). Of particular importance are the substates of tier 0 (CS0). Sperm whale MbCO exists in three different CS0 characterized by the stretch frequencies of the bound CO, A_0 at ~1966 cm^{-1}, A_1 at ~1945 cm^{-1}, and A_3 at ~1930 cm^{-1}. The much weaker positive bands above 2100 cm^{-1} represent IR absorption by the photodissociated CO in the heme pocket. The positions of the B bands are close to the value of free CO at 2143 cm^{-1}, which indicates weak binding; however, the narrow line widths of these bands imply well-defined positions (Braunstein et al., 1993). The A substates have slightly different structures, most clearly evidenced from the different angles of the CO dipole to the heme normal (Ormos et al., 1988; Moore et al., 1988). The band positions have been explained by electrostatic interactions of the CO dipole with the charge distribution in the heme pocket arising from the different protein structures (Oldfield et al., 1991). The rebinding monitored within the individual A substates is nonexponential in time, which clearly shows the existence of substates in lower tiers of the hierarchy (CS1 and lower). The A substates have markedly different rebinding kinetics, and their relative populations are sensitive to external conditions such as temperature, pressure (Iben et al., 1989; Frauenfelder et al., 1990), pH (Shimada & Caughey, 1982; Hong et al., 1990), solvent viscosity (Young et al., 1991), and solvent chemistry (Makinen et al., 1979; Hong et al., 1990).

(v) Owing to the structural heterogeneity of proteins, spectral bands are inhomogeneously broadened (Cooper, 1983; Ormos et al., 1990). Spectral and kinetic parameters can be coupled if they both depend on the same structural coordinate. This effect is known as kinetic hole burning (Campbell et al., 1987; Agmon et al., 1988; Ormos et al., 1990; Chavez et al., 1990; Steinbach et al., 1991).

3. EXPERIMENTAL PROCEDURES

3.1. The Approach

We have studied the effects of extended illumination on ligand binding with near-IR and mid-IR measurements using Fourier transform infrared spectroscopy in combination with temperature-derivative spectroscopy (TDS), a kinetic protocol that allows examination of thermally-activated distributed rate processes (Berendzen & Braunstein, 1990). The TDS technique yields information on how illumination affects the taxonomic substates in both the bound and photodissociated states. The protocol involves two steps, as described in Figure 1, where the time dependencies of the sample temperature (Figure 1a) and illumination (Figure 1b) are shown. The first step is the preparation of the sample by illumination. In the second step, the distribution of the rebinding rates is examined with the TDS method: The rebinding is monitored while the sample is heated from T_{min} to T_{max} linearly in time, so that the ramp temperature, T_R, is given by

$$T_R(t) = T_{min} + \alpha t \qquad (3)$$

where α is the heating rate. For most experiments, α = 3.125 mK/s. Depending on protocol, T_{max} was varied between 100 and 200 K. During heating, spectra are continuously taken at the rate of 1 spectrum/K. At low temperatures, only molecules with small activation enthalpies rebind. As temperature and time increase, the rebinding of molecules with higher barriers becomes appreciable. Figure

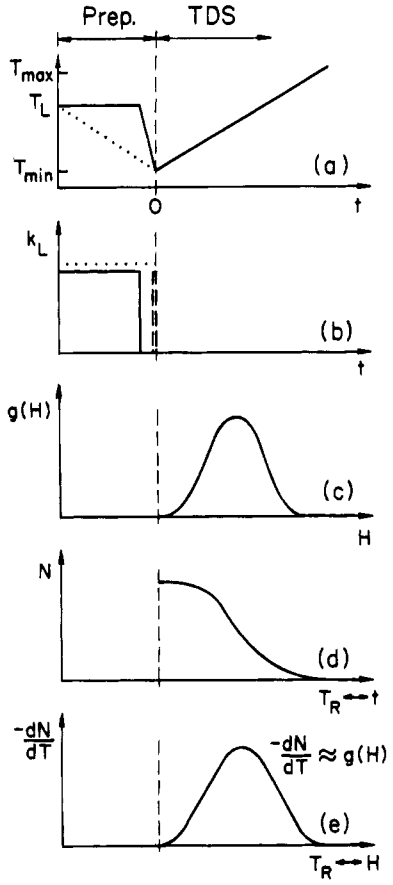

FIGURE 1: Schematic of temperature-derivative spectroscopy (TDS) protocols and analysis. (a) Time dependence of the sample temperature in TDS experiments. Proteins are illuminated for a time, t_L, at the temperature T_L. The sample is then cooled quickly to T_{min}, and the measurement is started. In "slow-cool" measurements (dotted line), the sample is cooled linearly in time from T_L to T_{min} under illumination. The measurement is then started at the time $t = 0$, and the sample temperature is ramped from T_{min} to T_{max}. (b) Time dependence of the sample illumination for TDS protocols. The dotted line refers to the illumination in "slow-cool" measurements. In experiments at a fixed illumination temperature, T_L (solid line), the sample is usually rephotolyzed with a short flash (5 s) before starting the TDS ramp. (c) Distribution of enthalpic barriers for ligand recombination, $g(H_{BA})$. (d) Temperature dependence of the photolyzed fraction, $N(t)$, for the enthalpy barrier distribution, $g(H_{BA})$. (e) Normalized, consecutive differences of spectra yield $-dN/dT_R$ as a function of ramp temperature, T_R. Given a pre-exponential, A_{BA}, the enthalpy barrier distribution, $g(H_{BA})$, can be extracted from this function; T_R is approximately proportional to an activation enthalpy.

1d shows the temperature dependence of the photolyzed fraction, $N(t)$, for an enthalpy barrier distribution, $g(H_{BA})$, as sketched in Figure 1c. The negative derivative of the photolyzed fraction with respect to the temperature, $-dN/dT_R$ (Figure 1e), closely resembles the distribution of rebinding barriers, $g(H_{BA})$.

To approximate the derivative, absorbance difference spectra, $\Delta A(\nu,T_R)$, are calculated from transmittance spectra, $I(\nu,T_R)$, at consecutive temperatures,

$$\frac{dA}{dT_R} \simeq \Delta A(\nu,T_R) = \log I(\nu,T_R - {}^1/_2K) - \log I(\nu,T_R + {}^1/_2K) \quad (4)$$

Taking the absorbance to be proportional to the concentration of the photolyzed species and normalizing yields $-dN/dT_R$.

We present TDS data in two different ways: either as contour maps of $\Delta A(\nu,T_R)$ (Figure 2) or as integrated absorbances, $\Delta A(T_R)$, as a function of T_R by integrating over the wavenumber region spanned by a particular substate. For instance, integrating from 1945 to 1950 cm^{-1} describes the rebinding of the A_1 substate. We call the corresponding cross-section an "A_1 slice".

TDS measures rebinding as a function of the ramp temperature, T_R. To convert T_R into an activation enthalpy, we use the fact that geminate rebinding is a first-order process and can be described by an Arrhenius relation, eq 2. T_R and the rebinding enthalpy, H, are related by (Berendzen & Braunstein, 1990)

$$H = RT_R \ln(A\tau_c) \quad (5)$$

where the characteristic time, τ_c, is given by

$$\tau_c = \frac{RT_R^3}{\alpha T_0(H + RT_R)} \quad (6)$$

If the pre-exponential, A, is known, eqs 5 and 6 can be solved numerically to connect H and T_R.

The illuminated state was prepared in two different ways. In some experiments ("slow cool"), the sample was illuminated as it was cooled down at a rate of 10 K/h from 160 to 12 K (dotted line in Figure 1a). In other experiments, we illuminated the sample at a constant temperature, $T_L >$ 12 K, for some time, t_L (solid line in Figure 1a), and then cooled down to 12 K in the dark at the highest possible rate. In most runs, a flash of 5 s ($k_L \simeq 5\ s^{-1}$) was applied at 12 K and then the TDS run was started. The purpose of the 5 s flash was to ensure complete photolysis, which allowed reliable normalization of different runs. In a few cases, there was no photolysis flash used and the TDS run was started immediately after the sample was cooled to 12 K.

We distinguish carefully between the illumination temperature, T_L, and the TDS temperature, T_R. T_L denotes the temperature at which the sample was exposed to light, whereas T_R gives the temperature at which a particular feature has been observed in the TDS map; T_R is approximately proportional to the activation enthalpy, H.

3.2. The Experiments

Freeze-dried sperm whale myoglobin and horse myoglobin were purchased from Sigma Chemical Co., St. Louis, MO, and used without further purification. The protein powder was dissolved in a mixture of 75% glycerol and 25% 1 M buffer solution (v/v). For samples with pH 6.0 or less, we used citrate buffers, above pH 6.0, phosphate buffers. The myoglobin was reduced with $Na_2S_2O_4$ solution prepared under anaerobic conditions and equilibrated with 1 bar of CO or O_2. The protein concentration of the samples was ~15 mM. For the measurements, a few microliters of the protein solution was kept between two sapphire windows (diameter, 13 mm), separated by a 75 μm thick mylar washer. The windows were sandwiched inside a block of oxygen-free high-conductivity copper that was mounted on the cold finger of a closed-cycle helium refrigerator (Model 22C, CTI Cryogenics, Waltham, MA), regulated with a digital temperature controller (Model DRC93C, Lake Shore Cryotronics, Westerville, OH).

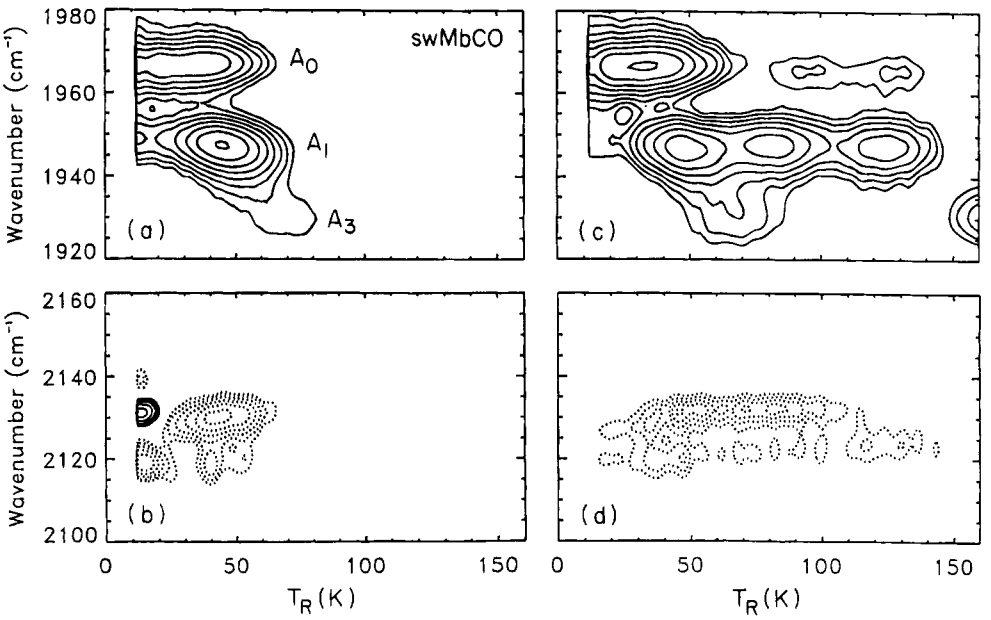

FIGURE 2: TDS contour maps of swMbCO (pH 6.0) recombination following photolysis with short and long illumination. Solid lines represent an increase in population; dashed lines represent a decrease in population. Consecutive differences of absorbance spectra, $\Delta A(\nu,T_R)$, are plotted as a function of the ramp temperature, T_R. (a) A states of swMbCO following complete photolysis (k_L = 5 s^{-1}; t_L = 5 s). Well-separated peaks of the rebinding signals of the three conformational substates (A_0, A_1, A_3) are observed. (b) B state contour map. Exchange between B substates occurs below ~20 K. Rebinding is indicated by the concomitant appearance of a positive signal in the A state contour map and a negative signal in the B state contour map. (c) A state contour map following slow cooling. Both A_0 and A_1 show three distinct rebinding peaks while A_3 shows only two. (d) Corresponding B contour map following cooling under illumination.

Transmittance spectra were collected on a Fourier transform infrared (FTIR) spectrometer (Model Sirius 100, Mattson, Madison, WI) between 1800 and 2300 cm^{-1} with a resolution of 2 cm^{-1} in the mid-IR and between 12 000 and 14 000 cm^{-1} with a resolution of 8 cm^{-1} in the near-IR. For each spectrum, 400 mirror scans were taken in 320 s.

The base lines of the difference spectra were fitted with a polynomial which was then subtracted. The areas and band positions of the CO stretch bands in the mid-IR were determined by fitting convolutions of Gaussians and Lorentzians to the spectra. The area of the near-IR band III near 760 nm (~13 000 cm^{-1}) was calculated from the absorbance, $\epsilon(\nu)$, as the zeroth moment, $M_0 = \int\epsilon(\nu)d\nu$. The band position, ν_{III}, was computed as the first moment, $M_1 = \int\epsilon(\nu)\nu d\nu/M_0$.

The samples were illuminated with light from an argon ion laser (Model 543, Omnichrome, Chino, CA). The laser was operated at 300 mW multimode output and emitted predominantly at 488 and 514 nm. The beam was split and focused with lenses on the samples from both sides. The standard photolysis rate coefficient k_L was determined at 12 K as ~20 s^{-1}. Lower photolysis rates were obtained by inserting calibrated neutral density filters into the beam.

4. RESULTS AND DISCUSSION

4.1. Overview

The TDS maps in Figure 2 provide an overview of the features encountered when illuminating a swMbCO sample for a long time. Figure 2a,b (A and B bands, respectively) shows contour maps from a TDS experiment started after a short flash (t_L = 5 s; k_L = 5 s^{-1}) at 12 K that completely photolyzed the sample. The solid lines in Figure 4a represent positive ΔA values and indicate increasing absorption in the A bands with time (and temperature), owing to recombination of the ligands. The peak of the A_0 signal at ~1966 cm^{-1} is located at slightly lower temperatures than that of A_1, whereas A_3 rebinds at markedly higher temperatures. These observations agree with the results of flash photolysis experiments (Steinbach et al., 1991; Young et al., 1991). Concomitant with the positive features in the A band map—except for an exchange at very low temperatures—negative features appear in the contour map of the B bands (Figure 2b), indicating rebinding of unbound CO molecules. The signal-to-noise ratio is smaller than for the A bands because of the smaller absorption of the photolyzed CO. We have recently determined the connections between the A and B substates (Mourant et al., 1993). The small shifts of the peak positions in both the A and B regions with temperature are caused by kinetic hole burning. They indicate a coupling between spectral and kinetic parameters (Campbell et al., 1987; Agmon, 1988). Essentially all CO ligands rebind below T_R = 90 K.

Figure 2c,d presents contour plots from a slow-cool experiment with the same sample illuminated (k_L = 20 s^{-1}) while being cooled from 160 to 12 K at a rate of 10 K/h before the TDS measurement was started (see Figure 1a).[1] This experiment shows the effects of extended illumination on the kinetic properties of the sample: a large fraction of the sample is still dissociated at 90 K. Instead of a unimodal distribution along the temperature axis, we observe three peaks for both A_0 and A_1 below 160 K. The fraction shifted to higher temperatures is considerably larger for A_1 and for A_0. For A_3, there are two peaks. Although the rebinding

[1] This experiment should not be confused with the cooling experiment proposed by Agmon and Hopfield (1983). They suggested cooling MbCO under intense illumination so that the heme would remain deligated and the protein would remain in the deoxy structure. Here we start with MbCO in the bound-state structure and study how this structure relaxes upon extended illumination.

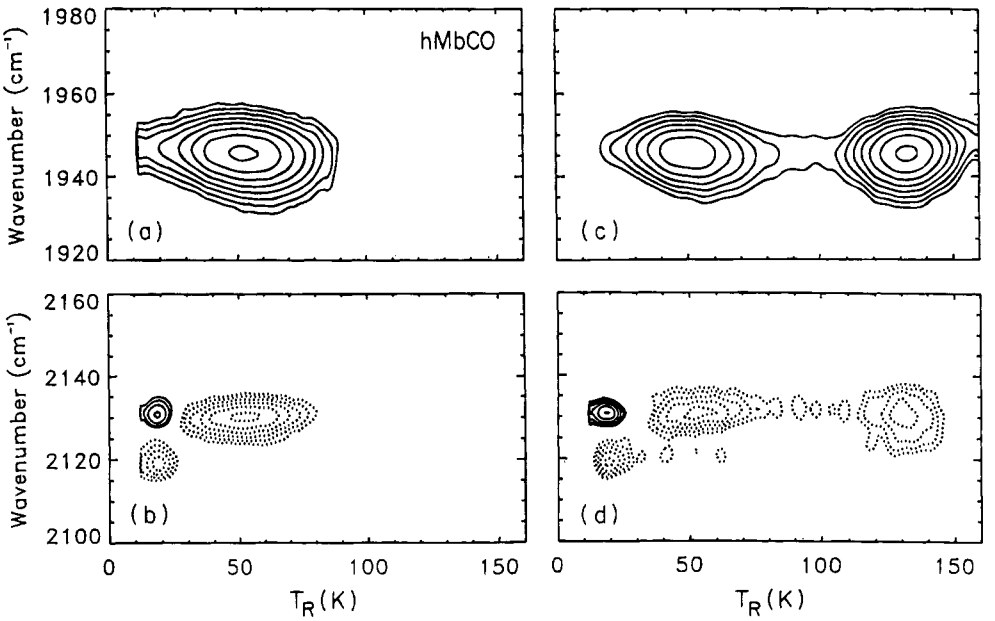

FIGURE 3: TDS contour maps of hMbCO (pH 6.8) recombination following photolysis with short illumination and slow-cool protocols. (a) Illumination for 5 s ($k_L = 5\ s^{-1}$). Only a single A substate, A_1 at ~1945 cm^{-1}, is appreciably populated. (b) B state contour map following short illumination. (c) A state contour map after slow cooling under illumination ($k_L = 20\ s^{-1}$). There are two pronounced rebinding peaks for A_1. A third peak at $T_R \simeq 80$ K is only weakly populated compared with swMbCO. (d) Corresponding B state contour map following cooling under illumination.

Table 1: Substates Created by Light-Induced Relaxation[a]

system	A substate	log(A_{BA}/s^{-1})	H_p (kJ/mol) unrelaxed B^0	relaxed B^1	B^2	B^3
swMbCO	A_0	8.7	7.5	7.9	21	30
	A_1	8.9	10.0	11.2	19	29
	A_3	10.4	17.4	17.6	–	41
hMbCO	A_1	9.2	11.9	12.1	–	32

[a] The peak enthalpies of the LIR substrates are calculated with eq 2 assuming the pre-exponential factors given in the Table.

properties change drastically, the fractional populations of the three A substates remain unaltered, in agreement with previous studies that show no exchange between the A substates below about 160 K (Iben et al., 1989; Frauenfelder et al., 1990; Mourant et al., 1993). Figure 2d shows the TDS map of the B bands after illumination. The spectral positions are very close to those in Figure 2b. As stated in section 3.1, T_R is approximately proportional to H. If we assume that the pre-exponential A does not change appreciably, the activation barriers for the shifted peaks of A_0 and A_1 consequently are about 20 and 30 kJ/mol (see Table 1). If the increase in barrier heights was due to a tighter binding of the CO at some docking site, we would expect a considerable change in the position of the B bands. The absence of such a shift suggests that the slowing of the CO rebinding is not caused by pumping of the CO to an alternative site but by a relaxation phenomenon. We call this effect "light-induced relaxation" or LIR.

Figure 2 suggests that the relaxation producing the higher barriers occurs in a few discrete hops and not as a continuous process. We interpret the peaks in the TDS maps in Figure 2 as taxonomic substates in the photodissociated state B. The unrelaxed peak (or substate) shall be denoted by B^0 and the three relaxed peaks in order of increasing activation enthalpies as B^1, B^2, and B^3. A complete characterization of these substates would, for instance, be $B^3 2119(A_1)$, indicating the third relaxed B substate at a wavenumber 2119 cm^{-1} rebinding to the substate A_1. If necessary, we add the subscript L or T to indicate that the B substate has been created by light or thermally.

The absence of a shift in the wavenumber of the photodissociated CO and the appearance of taxonomic (discrete) substates after illumination could be an accident in swMbCO. We therefore performed slow-cool experiments also with hMbCO. swMbCO and hMbCO have similar sequences, but 18 residues are different. If light were to pump the CO to different docking sites in the heme pocket, we would expect little changes in the bound-state spectra but pronounced changes in the spectra of the photodissociated CO. The result is just the opposite. The bound state of hMbCO displays mainly one A substate at pH 7, at 1945 cm^{-1}. A TDS experiment after a short flash shows only B^0 at $T_R = 54$ K (Figure 3a,b). Flash photolysis experiments of Post et al. (1993) show that this peak corresponds to an activation enthalpy of 12.1 kJ/mol. After slow cooling under illumination (Figure 3c), a very intense peak at $T_R = 133$ K appears. In analogy to swMbCO, we call this peak B^3. There is evidence for a small peak near 80 K that is prominent in swMbCO. The spectra in the photodissociated state (Figure 3d), however, show no significant change in the wavenumber on illumination.

The experiments with hMbCO confirm the two significant results of the swMbCO data: The slowing of the ligand binding appears to be due to a light-induced conformational relaxation of the protein and not due to a pumping of the CO to another site in the heme pocket. The relaxation appears to occur in discrete hops and not continuously. In the following, we will strengthen the evidence for LIR, investigate the main properties, and establish a connection between the light-induced and thermally-induced relaxation (TIR) observed earlier (Steinbach et al., 1991; Nienhaus et al., 1992).

4.2. Extended Illumination Induces Conformational Transitions

The experiments discussed so far have revealed little information about the structural changes that occur upon extended illumination. To obtain some insight into the structural aspects, we investigated band III, a weak absorption band in the near-IR (~13 000 cm^{-1}) that is only present in unligated myoglobin, either deoxy Mb or the photoproduct Mb*. It arises from a charge-transfer transition involving iron d-orbitals and porphyrin π-orbitals (Eaton et al., 1981; Makinen & Churg, 1983) and is therefore sensitive to the structure of the five-coordinated (high-spin) heme iron complex (Iizuka et al., 1974) but should not be affected by ligand motions in the distal pocket.

Band III is inhomogeneously broadened and shows kinetic hole burning (Campbell et al., 1987). Agmon (1988) has proposed that its wavelength should be proportional to the protein coordinate that determines the barrier height, H. We have found experimentally that the wavenumber, ν_{III}, of a homogeneous component and the rebinding barrier, H_{BA}, in photodissociated swMbCO are linearly related (Steinbach et al., 1991). Subsequently, we observed that thermal relaxation of the nonequilibrium photoproduct structure Mb*CO to equilibrium (deoxy) Mb above 160 K was accompanied by a shift of the position of band III by about 80 cm^{-1} to the blue (Nienhaus et al., 1992). This Mb* → Mb relaxation leads to a marked increase of the rebinding barriers (Steinbach et al., 1991). Lim et al. (1993) confirmed the blue shift of band III with picosecond resolution at room temperature. Obviously, band III is a superb marker for structural modifications near the heme iron.

To assess how the slowing of the kinetics produced by extended illumination is reflected in the position of band III, we collected TDS data in the near-IR using the same experimental setup as for the measurements in the mid-IR. Figure 4a shows the band position (first moment, ν_{III}) as a function of T_R for swMbCO at pH 6.6. Note that ν_{III} does not characterize the entire band III but only the fraction rebinding between T_R and T_R + 1 K. At pH 6.6, the swMbCO sample contains predominantly the A_1 substate. Photolyzing the sample with a short flash leads to an approximately linear relation between enthalpy, H_{BA}, and wavenumber, ν_{III}, with a slope of about 2.0 cm^{-1}/K. This observation agrees with our earlier data (Steinbach et al., 1991). For the illuminated sample, ν_{III} follows the short-illumination values up to 50 K. Above 50 K, however, the slope decreases. The results for hMbCO in Figure 4b show a similar behavior, a linear relation between ν_{III} and T_R after a short illumination in the entire observable range and a decrease of the slope for the illuminated sample above T_R ≃ 60 K. The results in Figure 4a,b, together with the TDS maps in Figures 2 and 3, provide strong support for the conclusion that the light-induced slowing of CO binding reflects conformational changes. Figure 4a shows that, after a short flash, substates with ν_{III} > 13 085 cm^{-1} have T_R > 60 K. Figure 2a demonstrates that only about 15% are in this class. After the slow-cool procedure, the population above ν_{III} = 13 085 cm^{-1} has increased to about 50%. The corresponding numbers for hMbCO are about 30% after the short flash and more than 70% after the extended illumination. Therefore, concomitant with the slowing of the rebinding upon extended illumination, ν_{III} increases, implying

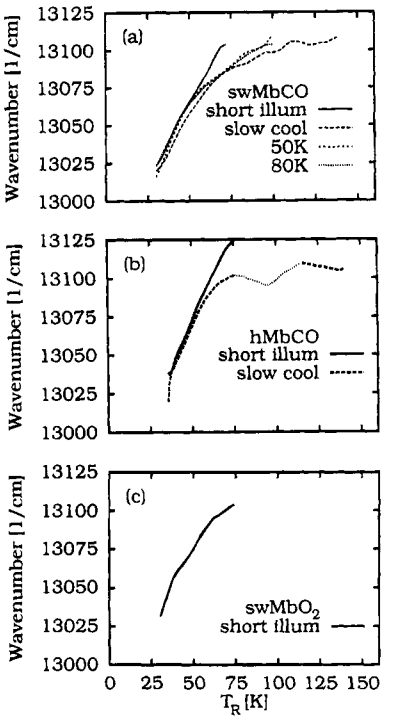

FIGURE 4: Position of band III, ν_{III}, from TDS experiments. The wavenumber ν_{III} is the first moment of band III of molecules that rebind at the TDS ramp temperature, T_R. (a) swMbCO, various illumination protocols: short illumination, slow cool from 160 to 12 K under illumination, and illumination for 10^4 s at constant temperature T_L = 50 and 80 K. (b) hMbCO, short illumination and slow cool from 160 to 12 K. The dotted line between 75 and 115 K indicates a region where only a small fraction rebinds; thus the error is rather large. (c) $swMbO_2$, short illumination. No changes were detected upon extended illumination of the sample at temperatures above 20 K.

that light induces conformational changes that modify the structure around the heme iron. Motion of the photodissociated CO in the heme pocket is unlikely to cause spectral shifts of the electronic transition.

The data in Figure 4 contain two more interesting results. The wavenumber of the illuminated sample does not appear to tend toward the value of 13 210 cm^{-1} for an equilibrium deoxy Mb sample. Moreover, the ν_{III}–T_R relations for MbCO and MbO_2 are quite similar.

4.3. Rebinding and Resetting

Do Mb molecules, after rebinding CO, remember that they were exposed to extended illumination? The experiments performed so far only give a limit: On the time scale of the TDS experiments, a few minutes, rebinding resets the original distribution. Two experiments, one with a short illumination, the other one with a long exposure followed by complete rebinding and then a short flash, give identical TDS maps. Therefore, the sample has completely recovered after recombination; no permanent changes occur in the sample even after high-intensity illumination for many hours.

4.4. Slowing Is Photon Induced

Ansari et al. (1987) postulated that the slowing of CO rebinding to swMb is due to the fact that light rephotolyzes MbCO repeatedly and that the system has a small probability to move to a longer-lived conformational substate after photodissociation. Here we will show that this model is wrong and that light plays a role beyond photolysis.

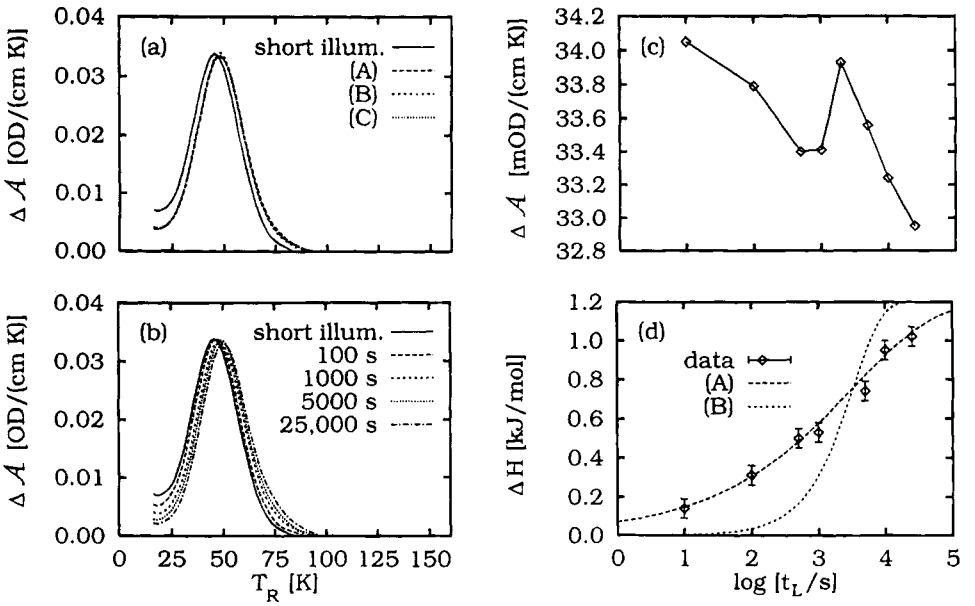

FIGURE 5: (a) Absorbance difference, $\Delta A(T_R)$, integrated between 1945 and 1950 cm^{-1}, following short illumination (25 photons per molecule) or long illumination (20 000 photons per molecule) of a swMbCO sample (pH 6.6) at 25 K. Long-illumination protocols are as follow: (A) 10^4 s with a $k_L = 2\ s^{-1}$, (B) 10^3 s with $k_L = 20\ s^{-1}$, and (C) a cycle of 1 s illumination ($k_L = 20\ s^{-1}$), 9 s darkness, repeated 10^3 times. (b) Absorbance difference for A_1, as a function of T_R, for various illumination times, t_L, at $T_L = 25$ K. (c) Peak height of the absorbance difference signal as a function of illumination time, t_L. (d) Shift of the distribution of $\Delta A(T_R)$ as a function of illumination time, t_L. Dashed line: fit to the data with a Kohlrausch function, $\Delta H(t)/\Delta H(\infty) = 1 - \exp[-(\phi^* k_L t_L)^\beta]$. Dotted line: exponential time dependence for comparison.

Photon Absorption by Photodissociated MbCO Slows Rebinding. To see if light changes the rebinding barriers directly or through rephotolysis, the effect is studied at low temperatures where most of the photolyzed proteins remain in state B. Friedman and co-workers (Ahmed et al., 1991) have observed a small light-induced slowing of rebinding even at 2 K. We performed our experiments at $T_L = 25$ K, where LIR is easily observable, but rebinding is still slow.

The data for the extended illumination at 25 K are presented in Figure 5a. The plots show the absorbance difference, $\Delta A(T_R)$, for the A_1 substate of swMbCO, obtained by integrating $\Delta A(\nu,T_R)$ between 1945 and 1950 cm^{-1}, as a function of TDS temperature, T_R. More than 90% of the molecules remain dissociated throughout the illumination phase even for illumination times $t_L \simeq 10^4$ s; only molecules with barriers below ~6 kJ/mol have shorter lifetimes. Thus at 25 K, barrier changes must occur while the molecules are in the photolyzed state. To account for the observed effects, one may invoke two different models: In a *thermal relaxation model*, the photolyzed proteins relax from a nonequilibrium state to an equilibrium state with higher barriers for rebinding. Extended illumination merely serves to keep a steady-state population in the B state. In a *photon-induced process*, light absorption is a key ingredient in the process that enables the molecules to change their rebinding barriers. As rebinding is negligible when illuminating at $T_L = 25$ K, the thermal relaxation model would imply that barrier shifts occur in the dark. We have kept samples in the dark for many hours after illumination before cooling to 12 K to start the TDS run and have only seen changes in the distribution caused by the rebinding of the CO while the sample sat in the dark. Therefore the slowing is not caused by a purely thermal relaxation that changes the barriers of the photolyzed Mb molecules, as has already been noticed by Friedman and collaborators (Ahmed et al., 1991).

The Light-Induced Relaxation Depends on the Number of Photons. To further prove the active involvement of photons, we illuminated the sample with the same number of photons ($n = k_L t_L = 2 \times 10^4$) at $T_L = 25$ K in three different ways: for 10^3 s with $k_L \simeq 20\ s^{-1}$, for 10^4 s with $k_L \simeq 2\ s^{-1}$, and with $k_L \simeq 20\ s^{-1}$ using a mechanical shutter that was opened for 1 s every 10 s. Figure 5a shows that the results are identical. Therefore, the magnitude of the LIR depends on the number of photons.

Even the Photolyzing Light Quantum Can Change the Distribution. The next question is whether the MbCO system must be in the photodissociated state B for LIR to occur. In other words, is it necessary for the system to absorb two photons, the first to photolyze, the second to change the conformation? This question can be answered at high temperatures, where rebinding is so fast that even under constant illumination the proteins are predominantly in the bound state. We illuminated MbCO at $T_L = 80$ K for 10^4 s with three different intensities corresponding to $k_L = 0.2$, 2, and 20 s^{-1}. Figure 6a shows the corresponding TDS slices. The solid vertical line, labeled $H(t_L)$, marks the enthalpy above which the molecules remain photolyzed throughout the entire illumination period, t_L. Molecules with lower barriers, which are the majority, recombine and are photodissociated several times during illumination. Recombination resets the molecules to the original (low-barrier) state; thus the effective time over which molecules at a particular enthalpy can be accumulated is shorter than t_L for molecules with barriers to the left of $H(t_L)$ and given by $1/k_{BA}$. The yield for generating molecules with these barriers may actually be quite high, but recombination prevents their accumulation. Consequently, the relaxed population decreases toward lower barriers.

The dashed line in Figure 6a is denoted with $H(k_L)$. Molecules with barriers lower than $H(k_L = 20\ s^{-1})$ rebind within the time $1/k_L = 50$ ms and spend only a fraction of

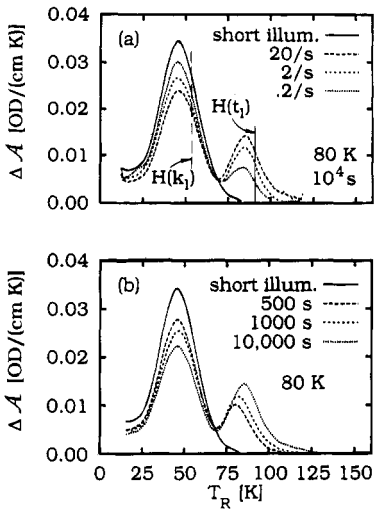

FIGURE 6: (a) TDS slices of A_1 of swMbCO (pH 6.6) after short illumination and illumination at T_L = 80 K, t_L = 10 000 s with full laser power and with 1 and 2 OD neutral density filters in the beam, corresponding to photolysis rate coefficients of k_L = 20, 2, and 0.2 s^{-1}. The solid line labeled $H(t_L)$ marks the enthalpy above which the molecules remain photolyzed throughout the entire illumination period, t_L. The dashed line marked $H(k_L)$ is explained in the text. (b) A_1 slices for short illumination and for t_L = 500, 1000, and 10 000 s.

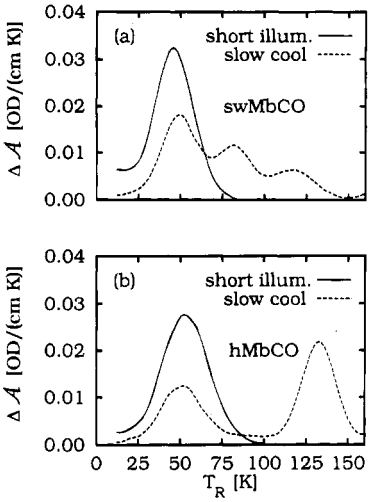

FIGURE 7: Short-illumination and slow-cool rebinding enthalpy distributions. (a) A_1 slices through the TDS contour map of swMbCO (pH 6.6) with short-illumination and slow-cool protocols. (b) Slices through the TDS contour map of hMbCO (pH 6.8) with short-illumination and slow-cool protocols.

the illumination time in the photolyzed (B) state. Photons will be absorbed predominantly by ligated molecules. In contrast, proteins with barriers higher than $H(k_L)$ stay photodissociated for most or all of the time. If a change of the rebinding barrier occurred *only* from absorption of a photon by an already photodissociated myoglobin molecule at T_L = 80 K, we would expect a low efficiency for molecules with barriers below $H(k_L)$, whereas the ones above $H(k_L)$ should exhibit a high efficiency. But we see no discontinuities in the missing population around $H(k_L)$. Therefore, we conclude that the photolyzing photon is already capable of inducing the relaxation. Figure 6a permits a quantitative proof. At 80 K, Mb molecules with activation enthalpies below the peak of the unrelaxed distribution (T_R = 43 K; H_p = 10 kJ/mol) rebind with rate coefficients k_{BA} > 200 s^{-1}. Under illumination with k_L = 0.2 s^{-1}, less than 10^{-3} of the Mb molecules with H_{BA} < 10 kJ/mol are in state B. If only molecules in state B would relax under illumination, the distribution for k_L = 0.2 s^{-1} would follow the unrelaxed curve up to about 50 K. The data show, however, that illumination lowers $g(H_{BA})$ down to less than 10 K or 2 kJ/mol. The conclusion is inescapable that the photons that photodissociate MbCO with unit quantum yield can, at the same time, also initiate a conformational transition but with a smaller quantum yield.

4.5. The Light-Induced Relaxation Occurs in Steps

To distinguish between continuous and stepwise relaxation, we performed experiments with different illumination times, t_L, shown in Figure 5b. At first sight, the distribution $g(H_{BA})$ appears to shift smoothly toward higher values. The data can, however, also be explained by a two-state transition where the observed distribution is the sum of two overlapping contributions peaked at two different activation enthalpies. The two cases can be distinguished experimentally: If the shift is continuous, the distribution retains its shape, in particular its width and height. In a two-state transition involving an unrelaxed and a relaxed state, the observed distribution gets broader and decreases in height until the unrelaxed and relaxed population are equal. After that, it narrows again and increases in height as the relaxed population increases further. The peak height as function of the illumination time, t_L, in Figure 5c shows the behavior expected for a two-state model up to 5 × 10^3 s. For longer illumination times, the peak decreases again. This decrease may be explained by a tail toward high barriers that grows at longer illumination times. As we will see below, this tail turns into a peak as we illuminate at temperatures around 80 K. The peak that can be generated by illumination at 80 K can thus already be populated at 25 K, although with much lower efficiency.

More evidence for stepwise relaxation comes from the slow-cool experiments shown in Figures 2 and 3. The absorbance differences, $\Delta A(T_R)$, for the A_1 substates in swMbCO and hMbCO are displayed in Figure 7. The slices demonstrate that the light-induced relaxation in swMbCO occurs in three steps through the substates B^1, B^2, and B^3. In hMbCO, only one relaxed substate is appreciably populated, and in analogy to swMbCO, we call it B^3.

Additional support for discrete states comes from a TDS experiment where the sample was prepared in three different ways (Figure 8): illumination for 5 s at T_L = 12 K; illumination for 10^4 s at 25 K and cooling to 12 K (A); and illumination for 10^4 s at 25 K, heating up to 80 K within a minute in the dark, and cooling down to 12 K (B). The TDS plot again shows the absorbance difference, $\Delta A(T_R)$, integrated between 1945 and 1950 cm^{-1}, for the A_1 substate as a function of TDS temperature. The temperature excursion to 80 K leads to rebinding of most of the population. The rebound molecules appear with the original distribution after rephotolysis at 12 K, whereas the molecules that remained photolyzed during the excursion still have their high-barrier values; they have not changed during the temperature excursion in the dark. Figure 8 shows that this population is missing from the center and the low-T_R side of the distribution (12 K ≤ T_R ≤ 50 K). In any continuous model with a single conformational coordinate (Agmon & Hopfield, 1983; Steinbach et al., 1991), the population that

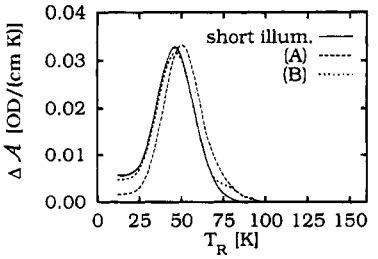

FIGURE 8: Discrete substates in the light-induced relaxation: A_1 slices through the TDS contour map (1945−1950 cm^{-1}) of swMbCO (pH 6.6) for a short-illumination protocol (solid line) and two long-illumination protocols. (A) The sample was illuminated for 10^4 s at 25 K. (B) The sample was illuminated for 10^4 s at 25 K and then quickly heated in the dark to 80 K and cooled to 12 K. Molecules that have rebound during the temperature excursion appear with their original enthalpy values after rephotolysis at 12 K.

still possesses high barriers would be missing from the high-barrier side. Proteins with small barriers would have no chance to relax. The relaxed distributions, for instance in Figure 6a, would coincide with the short-illumination curves at low T_R and deviate at high T_R, in contradiction with the experiments.

4.6. Photon Number Dependence of the LIR

Figure 5a shows that the LIR at 25 K depends only on the number, $n = k_L t_L$, of photons that impinge on the MbCO molecule but not separately on the intensity, k_L, or the duration, t_L, of the illumination. By measuring the LIR as a function of the illumination time and the intensity at two different temperatures, we will demonstrate here that the dependence on n holds not only at 25 K.

Illumination Time Dependence. Figure 5b shows that the activation enthalpy distribution appears to shift smoothly as a function of the illumination time, t_L. Figure 5d gives the shift of the apparent distribution as a function of t_L. We interpret the apparent shift as being caused by the transition between the unrelaxed substate B^0 and the relaxed substate B^1. If we assume that this transition is exponential in time and characterized by a single rate coefficient, we obtain the dotted curve in Figure 5d. Obviously, a single rate coefficient does not fit the data; the LIR is nonexponential in time. The shift can, however, be characterized by a stretched exponential function,

$$\Delta H(n)/\Delta H(\infty) = 1 - \exp[-(\phi^* n)^{\beta}] \qquad (7)$$

shown as a dashed line in Figure 5d. Here, $\Delta H(\infty) = 1.2$ kJ/mol is the maximum shift of the peak enthalpy. The exponent $\beta = 0.31$ characterizes the width of the distribution of rate coefficients for the transition from B^0 to B^1. The factor $\phi^* = 1.4 \times 10^{-5}$ gives an effective yield for the LIR.

The result obtained at 25 K is corroborated by data after illumination at $T_L = 80$ K with $k_L = 20\ s^{-1}$, shown in Figure 6b. To evaluate these data, we calculate the fraction, $p_2(n)$, of the initial distribution that has relaxed into the substate B^2 after exposure to n photons. To normalize $p_2(n)$, we assume that the slow-cool peaks in Figure 7 represent approximately the maximum fraction that can relax into a particular substate. In Figure 9, we plot log $p_2(n)$ versus log n. Also shown in Figure 9 is $p_1(n) = \Delta H(n)/\Delta H(\infty)$, using the data in Figure 5d.

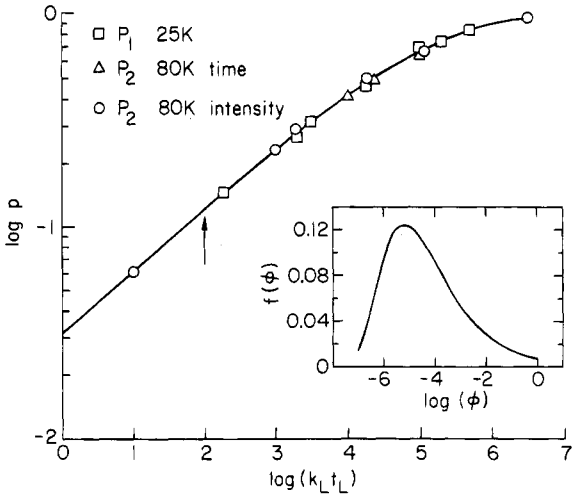

FIGURE 9: Dependence of light-induced relaxation on photon number: fraction of Mb molecules that have relaxed from B^0 to B^1, $p_1(t_L)$, and B^0 to B^2, $p_2(t_L)$, as a function of the number of incident photons, $n = k_L t_L$. The line is a stretched exponential fit to the data, with $\beta = 0.31$, $\phi^* = 1.4 \times 10^{-5}$. The arrow indicates the number of photons delivered by a nanosecond laser flash in a typical flash photolysis experiment. The inset shows the distribution, $f(\phi)$, of the quantum yield of relaxation, ϕ.

Intensity Dependence. Figure 6a shows the light-induced relaxation at 80 K for three different illumination intensities. Since the three illuminations all lasted 10^4 s, $H(t_L)$ is the same for the three experiments. To compare the fractions that have been relaxed into the substate B^2 at $T_R = 85$ K, we use the areas above $H(t_L)$. We normalize these areas by assuming that the slow-cool peaks in Figure 7 represent approximately the maximum fraction that can relax into a particular substate. The comparison indicates that, at $k_L = 20\ s^{-1}$ and $t_L = 10^4$ s, about 70% saturation is reached above $H(t_L)$. The normalized areas of the 80 K peak above $H(t_L) = 18.5$ kJ/mol for the three light intensities are shown in Figure 9. Figure 9 verifies the two observations made above, namely that the LIR depends only on the number of photons and that it is nonexponential in time. The time dependence expressed in eq 7 also fits the data in Figure 9.

The stretched exponential time dependence implies that the light-induced relaxation must be described by a distribution of quantum yields, $f(\phi)$, where $f(\phi)d\phi$ gives the probability of finding a quantum yield between ϕ and $\phi + d\phi$. The transition probabilities $p(n)$ can then be written as (Steinbach et al., 1992)

$$p(n) = 1 - \int f(\phi) \exp[-\phi n]\, d \log \phi \qquad (8)$$

The probability distribution $f(\phi)$ can be found numerically from the measured $p(n)$ by using eqs 7 and 8 (Lindsey & Patterson, 1980). The result is shown in the inset of Figure 9. Although the effective yield ϕ^* is very small, even a single photon ($n = 1$) has a non-negligible probability of causing a relaxation. Some distortion of the kinetics due to relaxation is consequently to be expected in nearly all experiments.

The peak position of the light-induced peak in Figure 6b shifts with t_L, but the curves merge at the low-enthalpy side. This behavior is expected because molecules with lifetimes short against the illumination times rebind many times during the illumination period. Their population is in a steady state, given by the ratio of the rate coefficients for production ($k_L \times \phi$) and depletion (k_{BA}). Mb molecules with activation

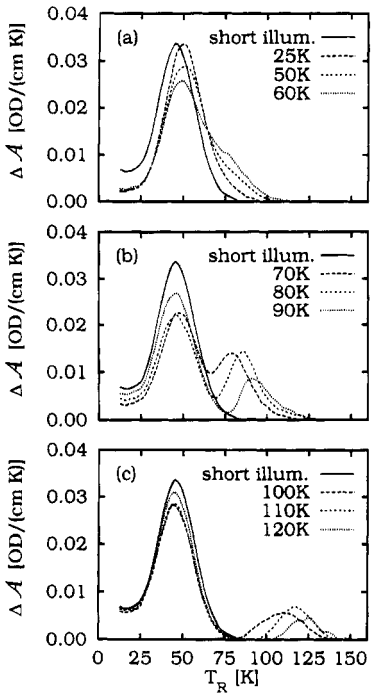

FIGURE 10: A_1 slices through the TDS contour maps (1945−1950 cm^{-1}) of swMbCO (pH 6.6) for $t_L = 10^4$ s at various illumination temperatures. For comparison, the short-illumination data are shown as solid lines.

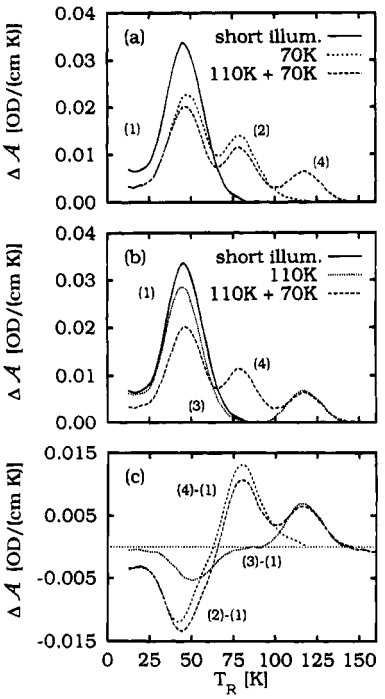

FIGURE 11: Mapping of the unrelaxed and relaxed distributions. swMbCO was illuminated with four different protocols: (1) 5 s at 12 K, (2) 10^4 s at 70 K, (3) 10^4 s at 110 K, and (4) 10^4 s at 110 K followed by 10^4 s at 70 K. Slices through the contour maps were taken at A_1. (a) Data for protocols 1, 2, and 4. (b) Data for protocols 1, 3, and 4. (c) Differences between the four runs reveal the mapping of the relaxation. The high-enthalpy barrier population of B^0 contributes to B^3 (curve 3 − 1), whereas the low-enthalpy barrier population of B^0 contributes to B^2 (curve 2 − 1).

enthalpies above $H(t_L) = RT \ln(At_LT/T_0)$, on the other hand, have lifetimes in the dissociated state that are longer than t_L. Their population increases steadily during illumination. The peak of the relaxed distribution that is populated after t_L occurs approximately at the ramp temperature corresponding to $H(t_L)$; it shifts to higher T_R with increasing t_L.

4.7. Temperature Dependence of the Light-Induced Relaxation in the A_1 Substate

To study the influence of the temperature, T_L, at which the sample is exposed to light, we performed a series of experiments with illumination at various temperatures with $k_L = 20\ s^{-1}$ and $t_L = 10^4$ s. Immediately after illumination, the sample was cooled in the dark and rephotolyzed with a 5 s flash at 12 K. In Figure 10, TDS slices, $\Delta A(T_R)$, for the A_1 substate are shown as a function of T_R, where again the absorbance difference, $\Delta A(\nu,T_R)$, has been integrated between 1945 and 1950 cm^{-1}.

Around $T_L \simeq 25$ K, the peak of the barrier distribution shifts from $T_R = 43$ to 48 K upon illumination. At 50 K, a long tail appears at the high-barrier side of the distribution which gets more pronounced at 60 K. At 70 K, the long tail seen at 50 and 60 K turns into a separate peak, B^2, at $T_R \simeq 80$ K. The peak at about 50 K is due to molecules that have been rephotolyzed at 12 K. B^2 gets even larger at 80 K but then decreases again at 90 K. Peak B^3 appears at $T_R \simeq 120$ K. The largest population in this peak is generated by illumination at 110 K. The high-barrier tail of this peak remains the same when illuminating between 120 and 140 K. Therefore, it appears that there are no more substates available with even higher barriers in the A_1 substrate. When illuminating near 160 K, additional features appear in the TDS maps that may be associated with solvent rebinding, thermal relaxation, or A substate exchange, as suggested by Berendzen and Braunstein (1990) and Šrajer et al. (1991). We do not consider these effects here.

The temperature series of experiments agrees with the results obtained on slow cooling under illumination, Figures 2, 3, and 7. Both types of experiments imply that the light-induced relaxation also involves a thermal component. It is striking that the peaks that appear while illuminating at a temperature, T_L, are characterized by temperatures, T_R, close to T_L.

4.8. Mapping of the Unrelaxed and Relaxed Distributions

In a continuous relaxation, the entire $g(H_{BA})$ distribution would shift to higher enthalpies under the influence of light without changing shape. Our experiments, however, present a different picture: As discussed in section 4.4 and shown particularly in Figure 8, the relaxation is not uniform; the high-barrier side of the relaxed distribution B^1 arises from the low-barrier side of the unrelaxed distribution B^0. We thus can ask if the substates B^2 and B^3 come from distinct parts of the unrelaxed distribution and if the relaxation occurs sequentially or in parallel. To answer these questions, we exposed the sample to light ($k_L = 20\ s^{-1}$) in four different ways: (1) 5 s at 12 K, (2) 10^4 s at 70 K, (3) 10^4 s at 110 K, and (4) 10^4 s at 110 K and then 10^4 s at 70 K (Figure 11). In the latter three runs, the sample was rapidly cooled to 12 K and rephotolyzed. Runs 3 and 4 show about the same B^3 population. This result is expected. The barriers are high enough that the subsequent illumination for 10^4 s at 70 K in run 4 does not lead to appreciable rebinding from B^3, and the yield to create B^3 at 70 K is insignificant. Run 4 shows less population in B^2 and also on the trailing edge of B^1 compared with the illumination at 70 K, run 2. If there were independent populations, one generating B^2 and the other

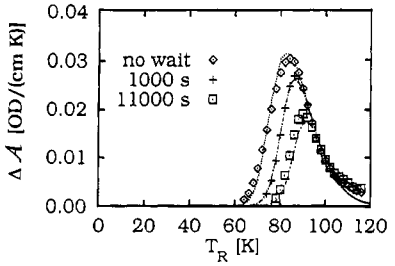

FIGURE 12: A_1 slices of swMbCO (pH 6.6) after illumination with $t_L = 10^4$ s, $T_L = 80$ K followed by waiting in the dark at 80 K for 0, 1000, and 11 000 s. The data reveal the inhomogeneity of B^2. The sample was not rephotolyzed after cooling from 80 to 12 K prior to the TDS experiment. The pre-exponential factor obtained is $\log(A_{BA}/s^{-1}) = 10 \pm 1$.

one generating B^3, we would expect the same population for B^2 in runs 2 and 4. The fact that the peak area is different indicates that at least some of the molecules can show up in either of these substates, with a probability that is strongly affected by the illumination temperature. After a significant fraction has relaxed into B^3, the population in B^2 decreases.

The data in Figures 10 and 11 indicate correlations between the normal and relaxed populations, which become particularly apparent when calculating differences between the four runs, Figure 11c. When populating B^3, the dominant part comes from the high-barrier side of B^0, whereas almost nothing gets lost from the low-barrier side. For B^2, the opposite effect is observed. As already mentioned, the measurements at 25 K indicate that the high-barrier side of B^1 is connected to the low-barrier side of B^0. The mapping between the initial substates, characterized by the low-temperature barrier H_{BA}, and the relaxed substates is consequently not simple and implies that the value of the shifted activation barrier is determined by more than one conformational coordinate.

4.9. Relaxations and Fluctuations

Linear response theory connects statistical fluctuations of a system in equilibrium with relaxations near equilibrium (Kubo, 1966). Therefore, one may ask if the light-induced relaxations observed in our experiments are also accompanied by fluctuations. The presence of fluctuations on time scales of the rebinding process or faster should lead to a narrowing of the rate distributions (Austin et al., 1975). Figure 7 shows that the relaxed peaks B^2 and B^3 in swMbCO and B^3 in hMbCO are nearly as broad as B^0, indicating that there are no fast fluctuations present. A direct proof of the non-exponential rebinding is given in Figure 12. In this experiment, swMbCO was illuminated at 80 K for 10^4 s. Subsequently, the sample was kept in the dark at that temperature for 0, 10^3, and 1.1×10^4 s. The fact that the substate B^2 represents an inhomogeneous distribution is evident because the population is depleted from the low-barrier side when keeping the sample in the dark after illumination. The conclusion is clear: Relaxation upon photon absorption occurs far from equilibrium and is not related to thermal fluctuations.

4.10. The Light-Induced Relaxation Is Sensitive to Structure

Light affects the three A substates differently. So far, we have focused on the behavior of A_1 in swMbCO because it can be studied most easily. A_0 and A_3, however, also display interesting features. Figure 4c shows two peaks for A_0, at positions similar to peaks B^2 and B^3 in A_1. The populations of these two substates are smaller than in A_1. The data do not permit us to say if a substate with small shift, analogous to B^1 in A_1, is present. The same remark holds true for A_3, where no conclusions regarding B^1 can be drawn. No substate corresponding to B^2 is visible, but a very strong peak appears in the TDS contour maps at $T_R = 160$ K. Obviously, the LIR is extremely sensitive to the different structures of the A substates.

The LIR in hMbCO. Figure 3c shows the effect of the extended illumination on the rebinding of CO to hMb. swMbCO and hMbCO differ. hMbCO displays mainly one A substate near pH 7, with a wavenumber similar to that of A_1 in swMb. LIR leads to an enormously strongly-populated substate, B^3, and $T_R = 133$ K, analogous to B^3 in swMbCO. B^1 is absent, and B^2 is only very weakly populated.

The LIR in swMbO₂. In contrast to MbCO, there is no good mid-IR marker available for MbO_2; therefore, we studied the near-IR band III. The dependence of the wavenumber, ν_{III}, on the rebinding barrier, H_{BA}, was examined with a TDS experiment. The data are shown in Figure 4c. Then we exposed the MbO_2 sample to light at different temperatures using identical conditions as for MbCO. While the sample was being illuminated, FTIR spectra were continuously taken. Generation of relaxed states should lead to an increase of the area of band III, indicating an increase of the photodissociated fraction. Illumination at 12 K leads to a tripling of the amount of photolyzed material when exposing the sample to about 10^4 photons per molecule compared to a short flash of about 5 photons per molecule. The additional photolyzed population rebinds at very low temperatures, mostly below 20 K, on the time scale of the FTIR spectrometer. When illuminating at temperatures above 20 K, where MbCO shows marked relaxation effects, neither spectroscopic nor kinetic changes were detected with MbO_2. The X-ray structures of MbCO (Kuriyan et al., 1986), MbO_2 (Phillips, 1980), and deoxy Mb (Nienhaus, 1987; Schlichting et al., 1994) may provide an explanation. In MbCO, the iron is in the mean heme plane when the ligand is bound, whereas in MbO_2 the iron is displaced toward the proximal side, normal to the heme plane, by 0.19 Å. In deoxy Mb, the displacement amounts to about 0.35 Å. After ligand dissociation at room temperature, a structural relaxation takes place that involves motion of the iron toward the proximal side. After photodissociation below 160 K, the iron shifts only partially out of the heme plane (Rousseau & Argade, 1986; Schlichting et al., 1994). For complete relaxation, the iron in MbCO must move 0.35 Å, but in MbO_2, the shift amounts to only 0.16 Å. Therefore, one should expect that the low-temperature photoproduct structure is less strained in MbO_2 than in MbCO and there may be less tendency for structural relaxations in MbO_2. These arguments are supported by studies that indicate that the Fe−His stretch frequency in the 80 K Raman spectrum of photodissociated MbO_2 is intermediate between that of deoxy Mb and photodissociated MbCO [Figure 4 of Ahmed et al. (1991)].

4.11. The LIR Increases the Activation Enthalpy

According to the Arrhenius equation, eq 2, the slowing of CO rebinding under extended illumination may be due to

an increase in the activation enthalpy (H_{BA}), a decrease in the pre-exponential (A_{BA}), or a combination of both. From TDS experiments at a fixed ramp rate, the influence of H_{BA} and A_{BA} cannot be disentangled. In this subsection, we use two different approaches to determine the pre-exponential for the relaxed substates and show that A_{BA} does does not change dramatically. Therefore, LIR predominantly leads to an increase in H_{BA} and not to a significant decrease in the pre-exponential factor.

Determination of A_{BA} by Using an Enthalpy Distribution. The first approach is based on the fact that the relaxed distributions are still inhomogeneous. Figure 12 shows that Mb molecules with small values of T_R rebind faster than those with large T_R. Equation 5 indicates that H_{BA} is approximately proportional to T_R. At a given temperature, we can therefore write for the rate coefficient of geminate rebinding

$$\log k_{BA} \simeq \log A_{BA} - \text{constant} \times T_R \qquad (9)$$

Determining the rate coefficient, k_{BA}, at a few values of T_R and plotting log k_{BA} versus T_R yield an approximate value of $\log(A_{BA}/s^{-1}) \simeq 8$ for the substate $B^2(A_1)$ of swMbCO. To obtain a more accurate evaluation, we note that dA/dT_R after a waiting time, t_w, at the temperature T is given by (Mourant, 1992)

$$\frac{dA}{dT_R} = \frac{C}{\beta}\int_{H_{min}}^{\infty} k(H,T_R)e^{-\Theta(H,T_R)}g(H)e^{-k(H,T)t_w}\,dH \qquad (10)$$

where

$$\Theta(H,T_R) = \int_{T_i}^{T_R}\frac{k(H,T')}{\alpha}\,dT' \qquad (11)$$

Fitting a suitable $g(H)$ to the data in Figure 12, and using eqs 2, 5, and 6, permits reproducing the data. Good agreement is obtained with $\log(A_{BA}/s^{-1}) = 10 \pm 1$.

Determination of A_{BA} by Changing the Heating Rate. Varying the heating rate affects the TDS signal. The faster the ramp rate, the higher in temperature molecules with given kinetic parameters, H_{BA} and A_{BA}, will rebind. The ramp rate dependence can be used to extract H_{BA} and A_{BA}. However, the changes are rather small for all practical heating rates. To obtain a large absolute temperature change for a given pair of heating rates, the experiment should be done at the highest temperature possible. Consequently, we chose B^3 in hMbCO. Using experimental data at two different heating rates (3.125 and 33.3 mK/s) and eqs 5 and 6, we solved the set of two equations for the two unknowns, H_{BA} and A_{BA}. The result is consistent with the assumption that the pre-exponential factor changes little during the light-induced relaxation. Assuming the same A_{BA} for the relaxed and unrelaxed substates, we obtain the activation enthalpies listed in Table 1.

The values in Table 1 show that the light-induced relaxation increases the activation enthalpies strikingly. The value for the substate $B^3(A_1)$ in swMbCO, about 29 kJ/mol, is similar to the value of 33 kJ/mol calculated by Agmon and Hopfield (1983). The barrier height for the substate B^3 in hMbCO, 32 kJ/mol, coincides with the value of 30 kJ/mol obtained by Post et al. (1993) for their thermally-relaxed state M.

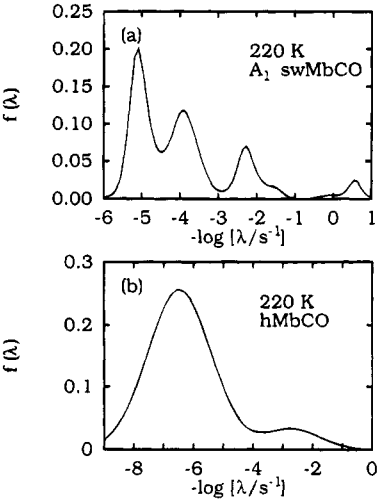

FIGURE 13: Connection between LIR and TIR. (a) Distribution of rebinding rate coefficients, $f(\lambda)$, at 220 K for A_1 of swMbCO. (b) Distribution of rebinding rate coefficients, $f(\lambda)$, at 220 K for hMbCO monitored in the Soret. Note the similarities with Figure 9.

4.12. Light-Induced and Thermally-Induced Relaxations Are Similar in MbCO

Flash photolysis experiments on swMbCO show a single, temperature-independent distribution of enthalpy barriers below 160 K. At higher temperatures, additional, discrete processes appear in the kinetics (Steinbach et al., 1991). These additional, slowly-rebinding populations are explained by a thermally-induced relaxation (TIR) that leads to much higher rebinding barriers. Using the maximum entropy method (Steinbach et al., 1992), the survival probability, $N(t)$, at each temperature can be converted into a rate distribution function, $f(\lambda)$, defined through

$$N(t) = \int f(\lambda)e^{-\lambda t}\,d\log\lambda \qquad (12)$$

Rebinding processes that are temporally separated show up as peaks in $f(\lambda)$. The enthalpy distributions from extended illumination experiments resemble the rate distributions from flash photolysis kinetics. In swMbCO, LIR is characterized by three peaks in A_0 and A_1 and two peaks in A_3 (Figure 2). The geminate rebinding shows the same pattern (Johnson, 1991). In hMbCO, LIR yields two pronounced peaks (Figure 3) and the flash photolysis rate distribution also has two peaks (Post et al., 1993). Post et al. have shown that the slowly-rebinding population in hMbCO can be enhanced by repeated flashing, consistent with our extended illumination experiments. Figure 13 gives examples for both swMbCO and hMbCO. The peak S in the flash photolysis kinetics represents rebinding from the solvent. This peak is not seen in the LIR experiments because they are done below the glass transition temperature of the solvent where the ligands cannot escape from the protein. The similarities in Figures 7 and 13 point to a fundamental connection between the populations created with the assistance of photons below ~160 K and the discrete populations generated thermally at higher temperatures.

Further support for the connection between LIR and TIR comes from the stretch band of the photodissociated CO in the heme pocket of hMb, measured under continuous illumination with $k_L = 20\ s^{-1}$ at 220 K and shown in Figure 14. Only the slowest rebinding fraction of the molecules

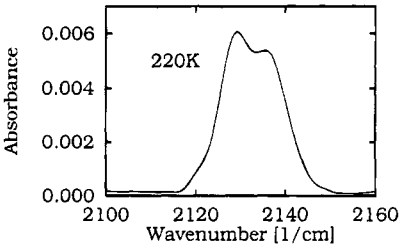

FIGURE 14: B substates in hMbCO under continuous illumination with $k_L = 20\ s^{-1}$ at $T_L = 220$ K.

remains unbound, and only a few ligands escape into the solvent. The IR spectrum of the photodissociated CO molecules in the heme pocket is essentially the same as that of the light-induced substate B^3 in Figure 3d. The agreement implies that the CO is still in the same position in the pocket as at low temperatures and has not moved to a new site. We have obtained analogous results also for swMbCO. Figure 14 poses the problem of the interpretation of the IR flash photolysis data of Austin and collaborators who report the disappearance of the B state absorption at 220 K within 600 ns after photodissociation (Hong et al., 1991). Our results imply that the B state signal persists on the millisecond time scale. We are unable to reconcile the observations.

The similarity between LIR and TIR is impressive for MbCO but does not extend to MbO_2. As discussed earlier, MbO_2 does not show a light-induced relaxation between 20 and 160 K. Earlier data, represented in Figure 13 of Steinbach et al. (1991), give clear evidence for a thermally-induced relaxation.

5. MODELS AND CONCLUSIONS

The experiments presented in the previous sections permit new insight into the structural and dynamic aspects of the ligand-binding reaction. In this section, we present a model that incorporates conformational relaxation and discuss possible structural features of myoglobin that give rise to the observed relaxation phenomena.

5.1. A Model for Ligand Binding

The binding of CO to Mb is a simple biological process. During the past few decades, a number of increasingly detailed models have been proposed, but the problem has not found an unambiguous solution. We mention only a few steps on the road to a "final" model. Initially, Mb + CO → MbCO was treated as a one-step process (Gibson, 1956; Antonini & Brunori, 1971). Low-temperature studies led to the proposal of a five-well model (Austin et al., 1975). This model reproduced the experimental data well but required a large number of parameters. Furthermore, it was static, with a temperature-independent reaction surface. Agmon and Hopfield (1983) pointed out that relaxation toward the deoxy structure after photodissociation should lead to a higher barrier for rebinding. Friedman and co-workers found evidence for such an effect in hemoglobin (Findsen et al., 1984; Friedman, 1985). Steinbach et al. (1991) introduced a shifting barrier distribution into the multiwell model. This model led to a reasonably successful description of ligand binding to swMb (Steinbach et al., 1991) and mutants of human Mb (Balasubramanian et al., 1993), but some peaks in the rate distribution, $f(\lambda)$, remained unexplained. Here we introduce a model that is based on

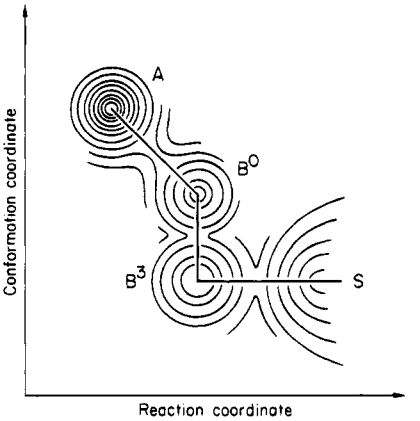

FIGURE 15: Schematic conformation−reaction surface for hMbCO. Rebinding from the solvent proceeds from S to state B^3. A conformational change of the protein−ligand pair is necessary to proceed to B^0. Finally, rebinding from B^0 to A involves the formation of a covalent bond between the ligand and the heme iron.

the similarity of LIR and TIR and accounts for the observed features.

Sperm whale myoglobin has served as a prototype for most in-depth discussions of ligand binding to monomeric heme proteins. However, the presence of the three A substates in swMbCO complicates a quantitative description of the binding process enormously. The barrier distributions, $g(H_{BA})$, of the three A substates are different (Ansari et al., 1987; Johnson, 1991), and the light-induced relaxation also differs for each of the A substates (Figure 2). Above about 180 K, transitions between the A substates further complicate the rebinding process (Frauenfelder et al., 1989; Young et al., 1991).

Ligand rebinding in hMbCO at pH ≃ 7 is dominated by a single A substate and has only one significantly populated relaxed substate, B^3 (Figure 3). Its kinetics are consequently simpler (Post et al., 1993), and we therefore describe the ligand-binding model for hMbCO. The key ingredient in this model is the identification of peak B^3 (and peaks B^1 and B^2 in swMbCO) with ligand rebinding in a conformationally-relaxed protein, in contrast to rebinding of a ligand that has moved away from the heme iron, as proposed earlier (Austin et al., 1975). We have presented several pieces of evidence for this interpretation: (i) Light-induced relaxation shifts band III to the blue, indicating changes in the geometry at the heme iron. (ii) The wavenumber of the IR absorption of the photodissociated CO in the heme pocket does not change under extended illumination, despite substantial changes in the rebinding barriers, implying that the CO does not move away from its B state position (Figures 2, 3, and 14). (iii) Light-induced and thermally-induced relaxation are similar (Figures 7 and 13). In particular, the light-relaxed substate, B^3_L, and the thermally-relaxed substate, B^3_T, show the same stretch band (Figures 3d and 14).

To describe the kinetics, we introduce the two-dimensional plot shown in Figure 15. Here the x-axis is a reaction coordinate, and the y-axis is a conformation coordinate. The reaction coordinate may be identified with the position of the CO: In S the CO molecule is in the solvent, in B it is in the heme pocket, and in A it is covalently bound to the heme iron. The CO does not move measurably during the relaxation $B^0 \rightarrow B^3$, and we indicate this fact by drawing the two substates along a vertical line. The conformation

coordinate reflects the structure of the protein molecule: In S the protein is in the deligated conformation, with the heme domed and the iron out of the mean heme plane. In A the heme is planar and the iron is in the mean heme plane. Crystallographic data of the individual B substates are not yet available, but some structural details can be inferred from spectroscopic experiments (see section 5.4).

With Figure 15, we can describe photodissociation and ligand binding at ambient temperature. The photodissociated MbCO system is initially in state B^0, with a barrier of about 12 kJ/mol. In this substate, rebinding would be very fast and few CO molecules could escape into the solvent. The relaxation $B^0 \rightarrow B^3$ increases the barrier to about 30 kJ/mol, large enough to "expel" most of the CO into the solvent. Relaxation, as proposed by Friedman (1985) (and called "self-induced trapping"), is crucial for the transition from the ligated to deoxy state. In ligand association, the CO enters the heme pocket from the solvent into the substate B^3. Since no permanent channel exists between the solvent and the pocket, the entrance can occur only because equilibrium fluctuations open transient pathways. From B^3, the CO can return to the solvent. In the binding step, the protein conformation changes simultaneously with the motion along the reaction coordinate. In swMbCO, the behavior is similar but the protein can undergo a series of conformational changes. Moreover, the protein can transit from one A substate to another, vastly complicating the quantitative treatment of the binding kinetics.

5.2. *A Model for the Relaxations*

Photodissociation leaves the protein initially in a nonequilibrium state close to the bound state, from where it subsequently relaxes either thermally at temperatures above ~160 K or induced by photon absorption below 160 K. An incident photon promotes the system to substate B^0. From there, it can either rebind or, at temperatures above about 160 K, thermally relax to B^3. A photon does, however, do more than just photodissociate; it also elevates the system into electronically-excited states. In the excited states, the enthalpy surfaces may look different, with smaller barriers than in the ground state and with shifted minima so that transitions to the substate B^3 become possible. The mechanism for the relaxation is not clear; breaking and reforming of hydrogen bonds may be involved.

In the temperature region around 200 K, separation of the relaxation intermediates into light-induced and thermally-induced substates is complicated by the fact that thermal relaxation and light effects may coexist. Light-induced substates, B_L, generated below 160 K, and relaxed substates above 160 K can be distinguished by their band III wavenumber. Only upon relaxation above ~160 K does the band shift to a position characteristic of equilibrium deoxy Mb (Nienhaus et al., 1992). A comparison of the activation enthalpies and entropies of the B_L and B_T substates is difficult because B_L and B_T are observed at different temperatures. Moreover, B_L is connected only to state A, while ligand escape into the solvent can occur from B_T. Preliminary data suggest that the barrier for rebinding may be smaller in B_L than in B_T. Apparently, the protein cannot fully relax at low temperatures where B_L is studied, while it is in the deoxy structure above about 160 K, where B_T is measured. We will give a structural explanation for this effect in section 5.4.

The conformational relaxation occurs in a discrete hop in hMbCO and in a few hops in swMbCO. No intermediate steps are observed. This remark requires some amplification because Figure 9 shows that the conformational transitions between the substates are nonexponential in time. We explain the nonexponentiality by a distribution of barrier heights, just as in the final binding step $B^0 \rightarrow A$. This assertion is supported by the results discussed in section 4.8, where we showed that the light-induced substates rebind nonexponentially and are characterized by a broad distribution of activation enthalpies. In this model, the relaxation $B^0 \rightarrow B^3$ in an individual protein is at any given time characterized by sharp activation parameters. The protein ensemble, however, is inhomogeneous and must be described by distributions.

5.3. *Homogeneous and Inhomogeneous Distributions*

The inhomogeneous distributions within the light-induced substates B_L raise the question of the nature of the thermally-populated substates B_T: Are they also inhomogeneous owing to the existence of conformational substates that interconvert slowly on the time scale of recombination, or are fluctuations fast enough to lead to an averaging, so that the ensemble appears kinetically as a single, homogeneous species?

Homogeneous and inhomogeneous distributions can in principle be distinguished by the multiple-flash technique (Austin et al., 1975; Frauenfelder, 1983). In a multiple-flash experiment, the sample is repeatedly photolyzed at fixed time intervals, chosen such that not all ligands have rebound before the next flash. In an inhomogeneous system, the survival probability, $N_i(t)$, after the ith flash in the same as the first, $N_i(t) = N(t)$. In a homogeneous system, successive flashes enhance the slowly-rebinding fraction.

The existence of a light-induced relaxation complicates the analysis of multiple-flash experiments. LIR promotes Mb molecules into substates with longer lifetimes and hence leads to a slowing in the multiple flash, thereby simulating a homogeneous system. This behavior neither proves nor excludes inhomogeneity within the light-relaxed ensemble of protein molecules. The original multiple-flash experiments by Austin et al. (1975) were performed at 70 K with few flashes so that the LIR was not detected, and the conclusion remains valid: The distributions at low temperatures are inhomogeneous; substates exist and are frozen. This conclusion is supported by the data shown in Figure 12.

At temperatures above about 160 K, the multiple-flash data are more difficult to analyze. Two groups (Tian et al., 1992; Post et al., 1993; Agmon et al., 1994) have performed multiple-flash experiments and claim that the high-temperature distributions are homogeneous. The results of the present paper imply that the data can also be explained by LIR.

Consider a double-flash experiment. First, the kinetics, $N_1(t)$, after a single flash is determined. In a second experiment, the first flash is followed by a second one after a delay, τ, and the kinetics after the second flash, $N_2(t)$, is measured. The difference, $\delta N(t,\tau) = N_2(t) - N_1(t + \tau)$, describes the kinetics of the proteins that have rebound a CO ligand during the time, τ, after the first flash. In an *inhomogeneous* system, $\delta N(t,\tau)$ will bind faster than $N_1(t)$ and will decay during τ. In the *homogeneous* case, however, $\delta N(t,\tau)$ will show the same time dependence as the entire

sample:

$$\delta N(t,\tau) = \text{constant} \times N_1(t) \quad (13)$$

Champion and collaborators (Tian et al., 1992) used a double-flash protocol at 264 K with a delay of $\tau = 80$ ns, found that $\delta N(t,\tau) \simeq$ constant $\times N_1(t)$, and concluded that the distribution giving rise to the observed nonexponential time dependence must be homogeneous. To discuss the experiment, we note that our model, Figure 15 for hMbCO and easily generalized to swMbCO, implies that rebinding can be written as

$$N_1(t) = (1 - x)N^f(t) + xN^s(t) \quad (14)$$

$N^f(t)$ characterizes the transitions from the unrelaxed substate B^0 which are fast. $N^s(t)$ describes the much slower transitions from the relaxed substates. The coefficient x characterizes the relative contributions of $N^s(t)$ and $N^f(t)$. The separation in eq 14 is valid if the fast transitions are completed after the time τ, so that $N^f(\tau) \simeq 0$, and if the slow ones change little during the time τ. Under these conditions, which are approximately satisfied for swMbCO at 264 K, $N_2(t)$ is given by

$$N_2(t) \simeq (1 - x)^2N^f(t) + x(1 - x)N^s(t) + xN^s(t + \tau) \quad (15)$$

and the difference becomes

$$\delta N(t,\tau) \simeq N_2(t) - N_1(t + \tau) = (1 - x)N_1(t) \quad (16)$$

According to the criterion eq 13, the system appears to be homogeneous. Thus the fast relaxation of the substate B^0 toward the substate B^3 simulates a homogeneous ensemble, and the experiment by Tian et al. does not decide if the distribution B^0 is homogeneous or inhomogeneous. The double-flash experiment also does not provide information on whether the relaxed substates B^2 and B^3 are inhomogeneously broadened.

Doster and co-workers (Post et al., 1993; Agmon et al., 1994) found that repeated flashing of hMbCO at 145 and 185 K enhances the population of a long-lived, broad state, M, and that the peak enthalpy of M increases on repeated flashing. They concluded that the state M must be homogeneous. Our results suggest a different interpretation. We identify their state M as the relaxed substate B^3 and propose that repeated flashing can increase the population of B^3 through light-induced relaxation. Since LIR and the standard multiflash enhancement of long-lived states are given by essentially the same algorithm, it is not surprising that they could quantitatively describe the enhancement of B^3. The observed increase in the peak enthalpy of B^3 is explained by the fact that longer illumination times lead to an enhancement of the population with higher barriers, as discussed in section 4.6 and shown in Figure 6b.

This discussion suggests that the two experiments claiming homogeneity are inconclusive. Indeed, two observations point to an inhomogeneous distribution: The geminate rebinding from B^3 is nonexponential in time from 180 to at least 220 K, and the widths of the LIR and the TIR distributions are similar up to about 210 K. The LIR distribution is clearly inhomogeneous, as was shown in section 4.8. It would be a surprising accident if another effect would lead to the same width for the TIR distributions. It is more likely that the width of both distributions is caused by the same effect, the existence of conformational substates that interconvert slowly on the experimental time scale. Additional experiments are needed to distinguish unambiguously between the two explanations, LIR or homogeneity.

At some temperature, fluctuations must average the rebinding rates and reduce the width of the distribution of B^3. Preliminary data suggest that the width of B^3 is constant to about 210 K. At 220 K, it is markedly reduced; above 220 K, the width is so narrow that good fits of the rebinding from B^3 can be obtained using an exponential. The width of the distribution for geminate rebinding $B^0 \rightarrow A$, however, remains large and essentially constant up to at least 250 K. These two observations indicate that the rates of the fluctuations that lead to a narrowing of the distributions lie between 10^4 and 10^7 s^{-1} at 250 K.

5.4. Structural Interpretation

Crucial for the interpretation of ligand binding is the understanding of the connection between kinetics, dynamics, and structure. Ideally, time-resolved structure determination, for instance using X-ray diffraction, could show how the protein molecules evolve after photodissociation. At present, this approach is still in a rudimentary stage. Fortunately, spectroscopic methods also supply structural information; they may even be sensitive to subtle structural changes that escape the resolution of crystallography. Infrared spectroscopy, resonance Raman (RR) scattering, X-ray absorption spectroscopy, and studies of electronic transitions, in particular of the conformation-sensitive band III near 760 nm, have yielded information on the structural details accompanying ligand binding. The pioneering RR work of Champion and collaborators (Bangcharoenpaurpong et al., 1984), Friedman and collaborators (Friedman et al., 1990; Ahmed et al., 1991), and Rousseau and collaborators (Rousseau & Argade, 1986) has created the basis for interpreting the kinetic data. The work of Friedman and collaborators, in particular, provides the background for the following discussion.

Various experiments imply that control and relaxation involve predominantly the proximal side (Doster et al., 1982; Smerdon et al., 1993). Figures 2 and 3 demonstrate that the IR absorption of the photodissociated CO is unchanged after illumination, suggesting that the structure on the distal side is not affected. Additional evidence comes from the work of Ahmed et al. (1991) who studied the intensity and the position of the iron−proximal histidine stretch band near 230 cm^{-1} in photolyzed MbCO with resonance Raman scattering after extended illumination. They found that the intensity of the stretch band, normalized to the fraction photolyzed, increased continuously between 2 and 200 K. They attributed this behavior to structural changes on the proximal side caused by the illumination.

Mechanisms for proximal control have been put forward by various groups (Šrajer et al., 1988; Friedman et al., 1990; Ahmed et al., 1991; Gilch et al., 1993; Schweitzer-Stenner et al., 1993; Stavrov, 1993). The iron is linked to the F helix through the proximal histidine (His F8). In deoxy Mb, the iron is markedly displaced from the heme plane (Nienhaus, 1987; Schlichting et al., 1994). To bind CO, the iron shifts from a position 0.35 Å away from the heme plane into the heme plane, and a major part of the rebinding barrier is

associated with the shift. Apart from electronic causes (Stavrov, 1993), steric repulsion between the imidazole side chain of the proximal histidine and the heme is responsible for the displacement of the iron.

The dominant steric repulsion is believed to arise from the contact between the C_ϵ proton of the His F8 imidazole side chain and the pyrrole nitrogen N_1. The strength of the interaction depends on the tilt angle, θ, of the Fe−His bond with respect to the heme normal and the azimuthal angle, ϕ, measured between the imidazole plane and the line connecting the pyrrole nitrogens N_1 and N_3. The two angles control the out-of-plane distance of the iron and hence the rebinding barrier. For minimal repulsion at a given tilt angle, the imidazole ring should be positioned at $\phi = 45°$. The more an eclipsing position ($\phi = 0°$) is approached, the more effective is the repulsion and the larger the rebinding barrier.

The geometry of the proximal histidine influences both the frequency and the intensity of the Fe−His stretch band. Friedman and collaborators (1990) suggest that the frequency is coupled to the tilt angle, θ, and the intensity to the azimuthal angle, ϕ, of the proximal histidine.

We now connect this model and the results of the LIR and TIR experiments. At low temperatures, the protein after photodissociation is in state B^0, still close to the bound-state structure, which corresponds to a small tilt angle, θ, and a large ϕ angle. In principle, photons can change both θ and ϕ. However, inspection of the myoglobin structure suggests that θ is less likely involved in the LIR because it cannot change unless the F helix shifts. As the F helix is in contact with the solvent, the tilt angle may only be able to change appreciably above the glass transition. Therefore, we assume that LIR changes the azimuthal angle in discrete steps to smaller angles, θ. The steric repulsion increases, and the barrier H_{BA} becomes larger so that bond formation is slowed. This scenario is supported by an increase of the intensity of the Fe−His Raman line (Ahmed et al., 1991) and by the partial shift of band III (Figure 4). In the thermally-induced relaxation, the same change in ϕ should occur. In addition, however, the tilt angle, θ, may also change because the F helix can move more freely above the glass transition of the solvent. This change can lead to an additional increase of the enthalpy barrier. Compared with hemoglobin, the F helix shifts only slightly in myoglobin, which may account for the small difference between LIR and TIR in hMbCO.

Flash photolysis experiments in solvents of different viscosities indicate that a large part of the protein participates in the thermally-induced relaxation (Beece et al., 1980). While the interpretation of the data has changed, the essential result remains unaffected: The relaxation steps $B^0 \rightarrow B^3$ depend on the external viscosity, indicating that some of the protein motions responsible for the increase in barrier height are coupled to the solvent. Additional, spectroscopic evidence for the coupling of conformational relaxation and solvent motions comes from flash photolysis experiments by Eaton and collaborators who studied the temporal evolution of the Soret band in solvents with different viscosities (Ansari et al., 1994).

5.5. Summary and Problems

The initial goal of the present work was to determine if the light-induced slowing of CO binding to Mb is caused by a conformational transition or by motion of the CO. The answer is now clear: A conformational, light-induced relaxation, mainly on the proximal side of the heme, increases the barrier for binding at the heme drastically. The light-induced relaxation shares similarities with the thermally-induced relaxation that takes place above about 180 K. A thermal relaxation had been predicted by Agmon and Hopfield (1983), and the experimentally-observed relaxation agrees in magnitude with the one calculated by Agmon and Hopfield. Some experimental features, however, differ from the theoretical model. In the Agmon−Hopfield model and its extensions (Agmon & Rabinovich, 1992; Agmon et al., 1994), the increase in activation enthalpy goes hand-in-hand with a narrowing of the rate distribution. Moreover, Agmon and collaborators treat both ligand binding ($B \rightarrow A$) and relaxation as diffusional motions. The experimental evidence indicates, however, that the relaxation $B^0 \rightarrow B^3$ does not homogenize the distribution and that motions along both coordinates are not diffusional but occur in a few discrete hops over distributed barriers.

The ligand-binding model displayed in Figure 15 can be treated quantitatively by a sequential scheme with four wells for hMbCO. We will present this analysis in a later publication. Generalization to swMbCO involves five sequential wells. It is amusing to note that such a five-well model is kinetically equivalent to the one originally proposed by us (Austin et al., 1975) and the relevant parameters for swMbCO can consequently still be used. The physical interpretation, however, is different. In the early model, the slowly-rebinding geminate states were interpreted as arising from binding sites of the CO in the protein matrix. The present work reveals that they are relaxed protein states, without significant motion of the CO.

The general features of protein dynamics that emerge from the present work are more important than the specific ligand-binding model. These features include the action of light in assisting or initiating protein relaxations, the observation that such relaxations occur in hops and are not continuous, and the fact that the relaxation rates differ in different substates. Moreover, the fact that the relaxed substates are still inhomogeneously broadened implies that the conformational substates are arranged in a hierarchy, thus supporting an earlier suggestion (Ansari et al., 1985).

The experimental results raise a number of new problems; we mention a few here. The relaxation induced even by the photolyzing flash poses the question if all earlier flash photolysis experiments have to be reanalyzed. The answer is most likely no. Particularly at low temperatures, the relaxation induced by the first flash is small. Nevertheless, it may be prudent to check the LIR by using different flash intensities. Multiple-flash experiments, however, have to be examined carefully to verify that thermally- or light-induced relaxations do not simulate a homogeneous ensemble.

One crucial, unsolved problem is the detailed connection between the structure and the dynamics in control of the ligand binding at the heme iron. More than one conformational coordinate is involved in the control (Šrajer et al., 1988). Figure 4 demonstrates this fact: The relation between the wavenumber, ν_{III}, and the activation enthalpy is very different for the unrelaxed and relaxed substates. Actually, three relevant parameters have been identified (Friedman et al., 1990; Gilch et al., 1993; Stavrov, 1993), the out-of-plane distance, c, of the iron, the tilt angle, θ, and the azimuthal angle, ϕ, of the proximal histidine. The detailed role of each,

their relaxation behavior, and their influence on spectral lines, for instance, on the position ν_{III} of band III, remain to be elucidated. A comparison of Figure 4a,c demonstrates that swMbCO and swMbO_2 exhibit essentially the same relation between ν_{III} and H_{BA} at low temperatures. Since MbCO and MbO_2 are known to have different average out-of-plane distances, ν_{III} and c are not uniquely related. Another problem that will require more studies is the elucidation of the mechanism of the light-induced and thermal relaxations. The exquisite sensitivity of LIR and possibly also TIR on structure and ligands suggests that an explanation must contain both general and structure-specific components. It also remains to be explored if LIR is important at ambient temperature and has biological consequences or if it is simply a low-temperature phenomenon that is useful for studying relaxations.

ACKNOWLEDGMENT

We are indebted to R. Ernst and R. Philipp for providing flash photolysis data on horse myoglobin. We thank B. Banko for expert assistance in computer programming and Y. Abadan, N. Agmon, J. Berendzen, W. Doster, D. Ehrenstein, C. Eng, R. Ernst, M. Filiaci, J. Friedman, B. McMahon, J. D. Müller, A. R. Panchenko, R. Philipp, and R. D. Young for helpful discussions and comments.

REFERENCES

Agmon, N. (1988) *Biochemistry 27*, 3507−3511.

Agmon, N., & Hopfield, J. J. (1983) *J. Chem. Phys. 79*, 2042−2053.

Agmon, N., & Rabinovich, S. (1992) *J. Chem. Phys. 97*, 7270−7286.

Agmon, N., Doster, W., & Post, F. (1994) *Biophys. J. 66*, 1612−1622.

Ahmed, A. M., Campbell, B. F., Caruso, D., Chance, M. R., Chavez, M. D., Courtney, S. H., Friedman, J. M., Iben, I. E. T., Ondrias, M. R., & Yang, M. (1991) *Chem. Phys. 158*, 329−351.

Ansari, A., Berendzen, J., Bowne, S. F., Frauenfelder, H., Iben, I. E. T., Sauke, T. B., Shyamsunder, E., & Young, R. D. (1985) *Proc. Natl. Acad. Sci. U.S.A. 82*, 5000−5004.

Ansari, A., Berendzen, J., Braunstein, D., Cowen, B. R., Frauenfelder, H., Hong, M. K., Iben, I. E. T., Johnson, J. B., Ormos, P., Sauke, T. B., Scholl, R., Schulte, A., Steinbach, P. J., Vittitow, J., & Young, R. D. (1987) *Biophys. Chem. 26*, 337−355.

Ansari, A., Jones, C. M., Henry, E. R., Hofrichter, J., & Eaton, W. A. (1994) *Biochemistry 33*, 5128−5143.

Antonini, E., & Brunori, M. (1971) *Hemoglobin and Myoglobin in Their Reactions with Ligands*, North-Holland, Amsterdam.

Austin, R. H., Beeson, K. W., Eisenstein, L., Frauenfelder, H., & Gunsalus, I. C. (1975) *Biochemistry 14*, 5355−5373.

Balasubramanian, S., Lambright, D. G., Marden, M. C., & Boxer, S. G. (1993) *Biochemistry 32*, 2202−2212.

Bangchaoenpaurpong, O., Schomacker, K. T., & Champion, P. M. (1984) *J. Am. Chem. Soc. 106*, 5688−5698.

Beece, D., Eisenstein, L., Frauenfelder, H., Good, D., Marden, M. C., Reinisch, L., Reynolds, A. H., Sorensen, L. B., & Yue, K. T. (1980) *Biochemistry 19*, 5147−5157.

Berendzen, J., & Braunstein, D. (1990) *Proc. Natl. Acad. Sci. U.S.A. 87*, 1−5.

Bonaventura, C., Bonaventura, J., Antonini, E., Brunori, M., & Wyman, J. (1973) *Biochemistry 12*, 3424−3428.

Braunstein, D. P., Chu, K., Egeberg, K. D., Frauenfelder, H., Mourant, J. R., Nienhaus, G. U., Ormos, P., Sligar, S. G., Springer, B. A., & Young, R. D. (1993) *Biophys. J. 65*, 2447−2454.

Brunori, M. J., Bonaventura, J., Bonaventura, C., Antonini, E., & Wyman, J. (1972) *Proc. Natl. Acad. Sci. U.S.A. 69*, 868−871.

Campbell, B. F., Chance, M. R., & Friedman, J. M. (1987) *Science 238*, 373−376.

Chance, B., Korszun, K., Khalid, S., Alter, C., Sorge, J., & Gabbidon, E. (1986) in *Structural Biological Applications of X-Ray Absorption, Scattering and Diffraction* (Bartunik, H. D., & Chance, B., Eds.) pp 49−71, Academic Press, New York.

Chavez, M. D., Courtney, S. H., Chance, M. R., Kiula, D., Nocek, H., Hoffman, B. M., Friedman, J. M., & Ondrias, M. R. (1990) *Biochemistry 29*, 4844−4852.

Cooper, A. (1983) *Chem. Phys. Lett. 99*, 305−309.

Dlott, D. D., Frauenfelder, H., Langer, P., Roder, H., & DiIorio, E. E. (1983) *Proc. Natl. Acad. Sci. U.S.A. 80*, 6239−6243.

Doster, W., Beece, D., Bowne, S. F., DiIorio, E. E., Eisenstein, L., Frauenfelder, H., Reinisch, L., Shyamsunder, E., Winterhalter, K. H., & Yue, K. T. (1982) *Biochemistry 21*, 4831−4839.

Eaton, W. A., & Hofrichter, J. (1981) *Methods Enzymol. 76*, 175−261.

Findsen, E. W., Friedman, J. M., Ondrias, M. R., & Simon, S. R. (1984) *Science 229*, 661−665.

Frauenfelder, H. (1983) in *Structure and Dynamics: Nucleic Acids and Proteins* (Clementi, E., & Sarma, R. H., Eds.) pp 369−376, Adenine Press, New York.

Frauenfelder, H., Parak, F., & Young, R. D. (1988) *Annu. Rev. Biophys. Biophys. Chem. 17*, 451−479.

Frauenfelder, H., Steinbach, P. J., & Young, R. D. (1989) *Chem. Scr. 29A*, 145−150.

Frauenfelder, H., Alberding, N. A., Ansari, A., Braunstein, D., Cowen, B. R., Hong, M. K., Iben, I. E. T., Johnson, J. B., Luck, S., Marden, M. C., Mourant, J. R., Ormos, P., Reinisch, L., Scholl, R., Schulte, A., Shyamsunder, E., Sorenson, L. B., Steinbach, P. J., Xie, A., Young, R. D., & Yue, K. T. (1990) *J. Phys. Chem. 94*, 1024−1038.

Frauenfelder, H., Sligar, S. G., & Wolynes, P. G. (1991) *Science 254*, 1598−1603.

Friedman, J. M. (1985) *Science 228*, 1273−1280.

Friedman, J. M., Campbell, B. F., & Noble, R. W. (1990) *Biophys. Chem. 37*, 43−59.

Gilch, H., Schweitzer-Stenner, R., & Dreybrodt, W. (1993) *Biophys. J. 65*, 1470−1485.

Hong, M. K., Braunstein, D., Cowen, B. R., Frauenfelder, H., Iben, I. E. T., Mourant, J. R., Ormos, P., Scholl, R., Schulte, A., Steinbach, P. J., Xie, A., & Young, R. D. (1990) *Biophys. J. 58*, 429−436.

Hong, M. K., Shyamsunder, E., & Austin, R. H. (1991) *Phys. Rev. Lett. 66*, 2673−2676.

Iben, I. E. T., Braunstein, D., Doster, W., Frauenfelder, H., Hong, M. K., Johnson, J. B., Luck, S., Ormos, P., Schulte, A., Steinbach, P. J., Xie, A. H., & Young, R. D. (1989) *Phys. Rev. Lett. 62*, 1916−1919.

Iizuka, T., Yamamoto, H., Kotani, M., & Yonetani, T. (1974) *Biochim. Biophys. Acta 371*, 1715−1729.

Johnson, J. B. (1991) Ph.D. Dissertation, University of Illinois at Urbana-Champaign, Urbana, IL.

Kleinfeld, D., Okamura, M. Y., & Feher, G. (1984) *Biochemistry 23*, 5780−5786.

Kubo, R. (1966) *Rep. Prog. Phys. 29*, 255−284.

Kuriyan, J., Wilz, S., Karplus, M., & Petsko, G. (1986) *J. Mol. Biol. 192*, 133−154.

Lim, M., Jackson, T. A., & Anfinrud, P. A. (1993) *Proc. Natl. Acad. Sci. U.S.A. 90*, 5801−5804.

Lindsey, C. P., & Patterson, G. D. (1980) *J. Chem. Phys. 73*, 3348−3357.

Makinen, M. W., & Churg, A. K. (1983) in *Iron Porphyrins, Part I* (Lever, A. B. P., & Gray, H. B., Eds.) pp 141−235, Addison-Wesley, Reading, MA.

Makinen, M. W., Houtchens, R. A., & Caughey, W. S. (1979) *Proc. Natl. Acad. Sci. U.S.A. 76*, 6042−6046.

Moore, J. N., Hansen, P. A., & Hochstrasser, R. M. (1988) *Proc. Natl. Acad. Sci. U.S.A. 85*, 5062−5066.

Mourant, J. R. (1992) Ph.D. Dissertation, University of Illinois at Urbana−Champaign, Urbana, IL.

Mourant, J. R., Braunstein, D. P., Chu, K., Frauenfelder, H., Nienhaus, G. U., Ormos, P., & Young, R. D. (1993) *Biophys. J. 65*, 1496−1507.

Nienhaus, G. U. (1987) Ph.D. Dissertation, Universität Münster, Münster, Germany.

Nienhaus, G. U., Mourant, J. R., & Frauenfelder, H. (1992) *Proc. Natl. Acad. Sci. U.S.A. 89*, 2902−2906.

Noks, P. P., Lukashev, E. P., Kononenko, A. A., Venediktov, P. S., & Rubin, A. B. (1977) *Mol. Biol. (Moscow) 11*, 1090−1099.

Oldfield, E., Guo, K., Augspurger, J. D., & Dykstra, C. E. (1991) *J. Am. Chem. Soc. 113*, 7537−7541.

Ormos, P., Braunstein, D., Frauenfelder, H., Hong, M. K., Lin, S.-L., Sauke, T. S., & Young, R. D. (1988) *Proc. Natl. Acad. Sci. U.S.A. 85*, 8492−8496.

Ormos, P., Ansari, A. Braunstein, D., Cowen, B. R., Frauenfelder, H., Hong, M. K., Iben, I. E. T., Sauke, T. B., Steinbach, P. H., & Young, R. D. (1990) *Biophys. J. 57*, 191−199.

Phillips, S. E. V. (1980) *J. Mol. Biol. 142*, 531−554.

Post, F., Doster, W., Karvounis, G., & Settles, M. (1993) *Biophys. J. 64*, 1833−1842.

Powers, L., Chance, B., Chance, M., Campbell, B., Friedman, J., Khalid, S., Kumar, C., Naqui, A., Reddy, K. S., & Zhou, Y. (1987) *Biochemistry 26*, 4785−4796.

Rabinovich, S., & Agmon, N. (1993) *Phys. Rev. E 47*, 3717−3720.

Rousseau, D., & Argade, P. V. (1986) *Proc. Natl. Acad. Sci. U.S.A. 83*, 1310−1314.

Schlichting, I., Berendzen, J., Phillips, G. N., Jr., & Sweet, R. M. (1994) *Nature* (in press).

Schweitzer-Stenner, R., Bosenbeck, M., & Dreybrodt, W. (1993) *Biophys. J. 64*, 1194−1209.

Shimada, H., & Caughey, W. S. (1982) *J. Biol. Chem. 257*, 11893−11900.

Smerdon, S. J., Krzywda, S., Wilkinson, A. J., Brantley, R. E., Carver, T. E., Hargrove, M. S., & Olson, J. S. (1993) *Biochemistry 32*, 5132−5138.

Šrajer, V., Reinisch, L., & Champion, P. M. (1988) *J. Am. Chem. Soc. 110*, 6656−6670.

Šrajer, V., Reinisch, L., & Champion, P. M. (1991) *Biochemistry 30*, 4886−4895.

Stavrov, S. S. (1993) *Biophys. J. 65*, 1942−1950.

Steinbach, P. J., Ansari, A., Berendzen, J., Braunstein, D., Chu, K., Cowen, B. R., Ehrenstein, D., Frauenfelder, H., Johnson, J. B., Lamb, D. C., Luck, S., Mourant, J. R., Nienhaus, G. U., Ormos, P., Philipp, R., Xie, A., & Young, R. D. (1991) *Biochemistry 30*, 3988−4001.

Steinbach, P. J., Chu, K., Frauenfelder, H., Johnson, J. B., Lamb, D. C., Nienhaus, G. U., Sauke, T. B., & Young, R. D. (1992) *Biophys. J. 61*, 235−245.

Tian, W. D., Sage, J. T., Šrajer, V., & Champion, P. M. (1992) *Phys. Rev. Lett. 68*, 408−411.

Winkler, H., Franke, M., Trautwein, A. X., & Parak, F. (1990) *Hyperfine Interact. 58*, 2405−2412.

Young, R. D., Frauenfelder, H., Johnson, J. B., Lamb, D. C., Nienhaus, G. U., Philipp, R., & Scholl, R. (1991) *Chem. Phys. 158*, 315.